

University of Southern Queensland
Faculty of Health, Engineering and Sciences

Land Subsidence Detection and Monitoring Using InSAR in Australia

A dissertation submitted by

Mr Jacob Cormick

In fulfilment of the requirements of
ENG 4111 and ENG4112 Research Project
Towards the degree of

Bachelor of Spatial Science (Honours) (Surveying)

Submitted October 2019

Abstract

The land surface is under constant movement in both horizontal and vertical directions. In some extreme circumstances there can be a sudden and significant subsidence event occur. These can be attributed to natural movement through earthquakes or through human intervention through extractive industries. Where these events occur, they can cause significant damage to the public infrastructure, housing and interruption to the people who live there. In some locations throughout Australia the disused underground mine sites are being developed into housing developments, particularly those close to urban areas such as Collingwood Park, Queensland. In the past in these there have been subsidence events occur and result in significant cost to the Government in damages.

Due to the high costs incurred with traditional monitoring techniques it has been cost prohibitive to provide ongoing monitoring to areas, where these events occur with long time periods separating the events. In more recent times through an increase of earth observation satellites with onboard Synthetic Aperture Radar (SAR) sensors have decreased the time period of acquisition. This has improved the results and reliability of the remote sensing technique known as Differential Interferometric Synthetic Aperture Radar (DInSAR). Therefore, making ongoing monitoring of these areas more economical which provides a significant benefit to these areas for ongoing monitoring.

This project conducted research into the detection and monitoring of Collingwood Park, Queensland located west of the city of Brisbane using the DInSAR technique. This site was chosen due to it having historically experienced subsidence events due to the collapse of the decommissioned underground mine. Due to its location it is an area where this type of research could be of great benefit and has the potential to provide the desired results.

The project used several data sets between the period of November 2015 to December 2018 acquired by the Sentinel 1A satellite which is part of the broader earth observation mission Copernicus. These data sets were obtained through Alaskan Satellite Facility Vertex system. The generated results indicate that no significant subsidence event had occurred during this time period and the area remained reasonably stable to June 2018. The results for the time period June 2018 to December 2018 do indicate some parts of the suburb had experienced some movement averaging around 0.008 meters of uplift for that area. Upon further processing it was indicated that this had occurred somewhere in the period of October to December 2018, this result was surprising as any movement in the area was expected to be subsidence.

University of Southern Queensland

Faculty of Health, Engineering and Sciences

ENG4111/ENG4112 Research Project

Limitations of Use

The Council of the University of Southern Queensland, its Faculty of Health, Engineering & Sciences, and the staff of the University of Southern Queensland, do not accept any responsibility for the truth, accuracy or completeness of material contained within or associated with this dissertation.

Persons using all or any part of this material do so at their own risk, and not at the risk of the Council of the University of Southern Queensland, its Faculty of Health, Engineering & Sciences or the staff of the University of Southern Queensland.

This dissertation reports an educational exercise and has no purpose or validity beyond this exercise. The sole purpose of the course pair entitled “Research Project” is to contribute to the overall education within the student’s chosen degree program. This document, the associated hardware, software, drawings, and other material set out in the associated appendices should not be used for any other purpose: if they are so used, it is entirely at the risk of the user.

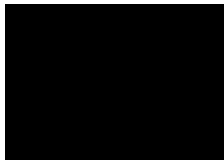
University of Southern Queensland
Faculty of Health, Engineering and Sciences
ENG4111/ENG4112 Research Project

Certification of Dissertation

I certify that the ideas, designs and experimental work, results, analyses and conclusions set out in this dissertation are entirely my own effort, except where otherwise indicated and acknowledged.

I further certify that the work is original and has not been previously submitted for assessment in any other course or institution, except where specifically stated.

J. Cormick



Acknowledgements

I would firstly like to thank my supervisor Dr Zahra Gharineiat for her guidance and advice throughout the course of the project.

Secondly, I would like to thank my family and friends for the continued support they provided whilst undertaking the degree. A special thankyou to my parents who helped make it possible for me to study fulltime and my sister who has endured me living with her for the past four years whilst studying.

Table of Contents

Abstract.....	2
Limitations of Use	3
Certification of Dissertation.....	4
Acknowledgements.....	5
List of Figures.....	8
1 Introduction	10
1.1 Project Background	10
1.2 Statement of Problem	11
1.3 Project Justification	11
1.4 Project Aim.....	11
1.5 Project Objectives	11
1.6 Summary.....	12
2 Literature Review	13
2.1 Introduction.....	13
2.2 What is InSAR?.....	13
2.2.1 Synthetic Aperture Radar (SAR)	13
2.2.2 Space Segment.....	14
2.2.3 Radar Polarisation	17
2.3 Interferometric Synthetic Aperture Radar	18
2.3.1 Image Selection.....	18
2.3.2 InSAR Processing.....	19
2.3.3 Differential InSAR	22
2.3.4 Phase Unwrapping	23
2.3.5 Noise Filtering	24
2.4 Applications of InSAR.....	24
2.4.1 Geomorphology	25
2.4.2 Hydrology	25
2.4.3 Infrastructure monitoring.....	25
2.5 Land Movement Detection	25
2.5.1 Traditional Techniques.....	25
2.5.2 DInSAR Studies.....	26
2.6 Conclusion	27
3 Methodology.....	29
3.1 Introduction.....	29
3.2 Data Acquisition and Image Selection	29

3.3	Processing	30
3.3.1	Coregistration.....	30
3.3.2	Coregistration check.....	34
3.3.3	Interferogram Generation.....	35
3.3.4	TOPSAR-Deburst	36
3.3.5	Create Subset of the area of interest	36
3.3.6	Topographic Phase Removal.....	37
3.3.7	Multi-look function	37
3.3.8	Goldstein Phase Filtering	38
3.3.9	Phase Unwrapping	39
3.3.10	Phase to Displacement	40
3.3.11	Terrain Correction.....	41
3.3.12	Coherence Masking.....	42
3.4	Stable point identification	42
4	Results and Discussion	44
4.1	Introduction.....	44
4.2	DInSAR Results	45
4.2.1	15-Nov-2015 to 19-Apr-2016	46
4.2.2	19-Apr-2016 to 03-Dec-2016.....	47
4.2.3	03-Dec-2016 to 13-Jun-2017	48
4.2.4	13-Jun-2017 to 22-Dec-2017	49
4.2.5	22-Dec-2017 to 20-Jun-2018	50
4.2.6	20-Jun-2018 to 29-Dec-2018	51
4.2.7	20-Jun-2018 to 18-Oct-2018	53
4.2.8	18-Oct-2018 to 29-Dec-2018	54
4.3	Conclusion	55
5	Conclusion and Further Research	57
5.1	Conclusion	57
5.2	Further Research	58
6	References	59
	Appendix A.....	62
	Appendix B	63

List of Figures

Figure 1 InSAR Bands Interaction with different surface: ESA Radar Course 2 (European Space Agency, 2019).....	14
Figure 2 Outline of SAR Satellite Missions (UNAVCO, 2018).....	15
Figure 3 Sentinel 1 Image acquisition modes (European Space Agency, n.d)	16
Figure 4 IW TOPSAR scan pattern (Yague-Martinez et. al, 2016).....	17
Figure 5 Effects of topography on SAR signal (Pinel, poland & Hooper, 2014)	18
Figure 6 Example of basic DInSAR (Sousa & Bastos, 2013).....	23
Figure 7 Alaskan Satellite Facility - search parameters (ASF, 2019).....	29
<i>Figure 8 S1 TOPS Coregistration overview</i>	<i>31</i>
<i>Figure 9 Subswath, polarisation & bursts selection (Master).....</i>	<i>32</i>
<i>Figure 10 DEM selection for coregistration.....</i>	<i>33</i>
Figure 11 ESD Parameters.....	34
<i>Figure 12 RGB output product</i>	<i>34</i>
Figure 13 Interferogram processing parameters	35
Figure 14 Example of image prior to deburst processing	36
<i>Figure 15 Geo Coordinates for area of subset</i>	<i>36</i>
<i>Figure 16 Topographic phase removal parameters.....</i>	<i>37</i>
Figure 17 Multi-look Parameters	38
Figure 18 Goldstein Filter parameter selection.....	39
Figure 19 SNAPHU export parameters	39
<i>Figure 20 SNAPHU Input parameters.....</i>	<i>40</i>
Figure 21 Terrain correction processing parameters.....	41
Figure 22 Coherence masking properties.....	42
Figure 23 Mining area (Ipswich City Council, 2018).....	44
Figure 24 Location of >0.97 coherence over time, Redbank plaza.....	45
Figure 25 Results Nov15-Apr16 White polygon represents area of interest, a coherence mask of 0.4 has been applied to the image.	46
Figure 26 Results Apr16 - Dec16 coherence masking of 0.4 was used for the output of this image. ..	47
Figure 27 Results for Dec16 - June17.....	48
Figure 28 Results for Jun17 - Dec17	49
Figure 29 Results for Dec17 - June18.....	50
Figure 30 Results for Jun18 - Dec18	51
Figure 31 Area of movement >0.006m with coherence value >0.6 shown by red pins.....	52
Figure 32 Results for Jun18 to Oct18	53
Figure 33 Results for Oct18 to Dec18	54

Figure 34 Area of movement $>0.006m$ with coherence value >0.6 55

1 Introduction

1.1 Project Background

Land movement can occur in any direction; however, this project is focused on the detection and monitoring of subsidence over time. Land subsidence which is the downward movement of the land surface can be caused by several factors, some of these being natural such as those surrounding fault zones while others are attributed human activities such as mining and water extraction.

The detection and ongoing monitoring of land deformation it is traditionally done with terrestrial survey techniques in a point measurement system. These techniques include the use of precise levelling whilst providing results accurate to millimetre level, it is a very time demanding method. In recent times GNSS techniques are commonly used which provide results with significant accuracy for monitoring the surface deformation. Whilst this method is quicker and physically easier it still has both high financial and time costs associated with these techniques. Due to the time and financial constraints with these traditional methods, there has been little to no ongoing monitoring available to areas which have had these events.

In more recent time, the use of a space based remote sensing technique has become more available and accessible with results showing good comparison to traditional techniques. This system is known as Interferometric Synthetic Aperture Radar (InSAR). It has added advantages over the traditional techniques which include the noncontact all weather application which reduces costs and has a greater spatial resolution which allows for monitoring of the surrounding area, resulting in a clearer understanding of the land movement.

The Ipswich region had a long history of coal mining which reportedly started in 1848 with several mines in production by 1890 and lasted until 1997. The two general methods for mining the coal was tunnelling or vertical shafts. It is reported that only 9% of the area is affected by the mining operations of which 1% has been developed into the urban area (Ipswich City Council: Planning Scheme Fact Sheet no.2, 2008).

Collingwood Park is an area that contained two underground mines known as Westfalen Number 3 and New Redbank Collieries. These mines began operation in 1965 and continued until they were decommissioned in 1987. This area has since been developed into a residential area. The method used in these was a board and pillar method mining at the depths of 60-140m (Shen et al.).

The area has experienced two subsidence events the first was in 1989 and the second in April 2008. The second event caused not only a change in land formation but also damage to existing properties and

structures in the area. The latest event has had a significant cost for the Queensland Government in compensation and acquiring the affected properties.

1.2 Statement of Problem

The traditional methods while providing a known accuracy, they do not provide the spatial resolution required to provide a description of the total deformation occurring and therefore have a limited use especially in prediction modelling (Yang & Peng, 2015). These methods also have a large associated cost which makes them prohibitive for monitoring large areas as well as for ongoing monitoring. Due to these limitations of the traditional technique's subsidence detection has typically been a reactive response to the issue rather than a proactive detection, the use of InSAR could have potential to be a proactive measure.

1.3 Project Justification

The current literature shows that this technique is a feasible method for the monitoring of land subsidence. However, there is an opportunity for further research to be conducted into the use of Sentinel satellite data in Australia. The use of InSAR in Australia has only had a small amount of research done into its use, specifically Sentinel 1. Given the consistent and short time periods for revisit over the same area it allows for a better temporal resolution that has not been available in past studies.

Using the remote sensing technique is a much more affordable solution to the problem as it is a non-contact all weather operation and the required data to undertake the analysis is freely available from the European Space Agency (ESA). The open source software from the European Space Agency, Sentinel-1 toolbox program SNAP will be used for processing the data.

It would provide benefits to those areas such as Collingwood Park where subsidence is ongoing and would benefit from a method that allows a cost-effective method for ongoing monitoring.

1.4 Project Aim

This project aims to investigate the use of space based InSAR using open source data and processing software for the purpose of detecting and monitoring subsidence occurrence in Queensland.

1.5 Project Objectives

The project objectives which have been identified in project specification in Appendix A, are listed below.

- Research the existing use of InSAR in the detection and monitoring of land subsidence.
- Establish background knowledge on the required processing techniques and software.
- Research and identify possible error sources with the using InSAR for subsidence, use previous SAR as validation.

These above objectives will be met through the undertaking of the literature review and required training/tutorials available from ESA and NASA.

- Identify a suitable area to conduct the monitoring, using a site where subsidence events are known to occur.
- Obtain the appropriate data from the European Space Agency (ESA) data hub.
- Analyse results from the SAR images to draw conclusion of the subsidence in selected area.
- Display the obtained results in an easily interpretable visual model.
- If time permits, a development model for prediction of future land subsidence events.

It is expected the above objectives will be met through the creation of velocity maps formed from the development of interferograms, this project is looking at the subsidence of land. From these results, an analysis will be of results was formed as to the total subsidence and the rate at which it is occurring. With time and resources permitting a model to predict future subsidence will be developed with the assistance of academic staff.

1.6 Summary

The dissertation is structured around five main chapters. Chapter 1 introduces the background to the dissertation topic as well as the aim and objectives for the project. Chapter 2 presents the review into current literature and what the techniques as well as other applications. Chapter 3 provides the methodology that is required for the project. Chapter 4 documents the results and discussion on the results. The last being chapter 5 which will provide conclusion and recommendations for further research.

2 Literature Review

2.1 Introduction

This chapter begins with a brief overview of the system and its components before moving onto to review of the applications for which it can be used. A review of previous studies will then be undertaken to identify where the knowledge gaps are and the potential errors as well as the accuracies that can be expected when using InSAR. The final section will outline the important factors that this project needs to follow or overcome to be successful in reaching part of the objectives.

2.2 What is InSAR?

2.2.1 Synthetic Aperture Radar (SAR)

Synthetic Aperture Radar (SAR) is an active remote sensing system that is usually space based on satellite but can also be based on aircraft or Unmanned Aerial Vehicles (UAV). Being an active sensor used on airborne platforms makes this system very attractive to earth surface observations for various land movements applications, flood modelling, and many other applications, as it can be utilised in all weather and lighting conditions.

The radar utilises microwaves in varying frequency and wavelengths, with the three most common being X, C, and L band, which have wave lengths of 3.1cm, 5.6cm and 23.5cm respectively. These microwaves are used to illuminate the earth's surface, the antenna then receives the returned signal which known as backscatter, containing both amplitude and phase components of the wave. The length of the waves effects its useability and purposes for which they suit, C band is more effective in slow rate deformation while L band was more suited to quicker subsidence or areas that have high levels of vegetation (Chatterjee et al. 2015). Figure 1 demonstrates how different bands penetrate different surfaces.

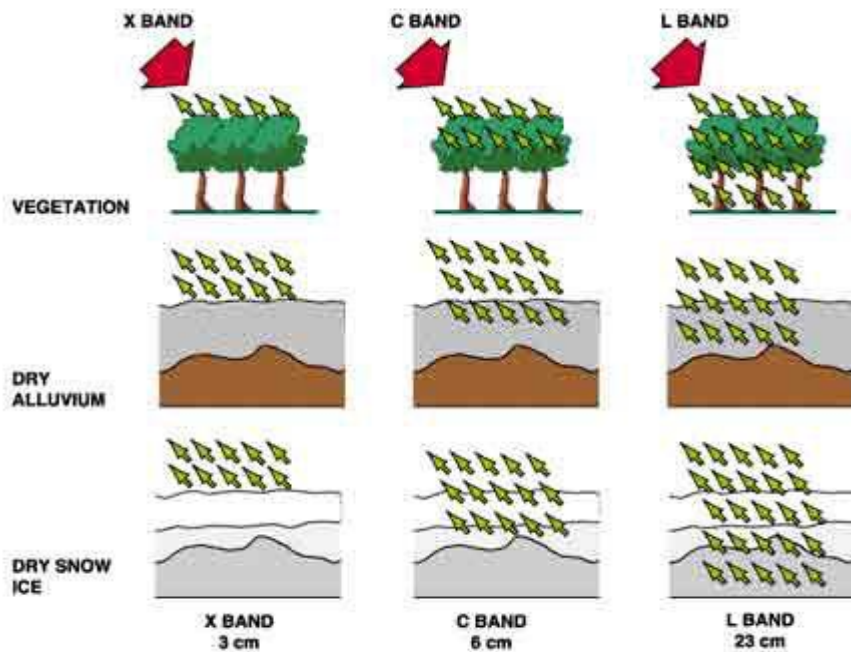


Figure 1 InSAR Bands Interaction with different surface: ESA Radar Course 2 (European Space Agency, 2019)

The signal returned contains two properties being amplitude and phase, Osmanoglu et al. (2015) describe the amplitude strength as being related to the shape, orientation, and electrical properties of the target. The phase component is the recording of the wave lengths to determine the time it takes for the signal to be returned. The processing of the raw SAR images will inevitably depend upon the application, the amplitude can be taken advantage of for use in hydrology studies whereas the phase of the wave is used for displacement.

2.2.2 Space Segment

There are a variety of satellite missions which have been used in the past and many more currently in use and into the future. Both C and L band sensors were some of the earliest utilised but in more recent time X band missions have come on board. Figure 2 below shows that as the technique has become more accepted many more satellites have become available.

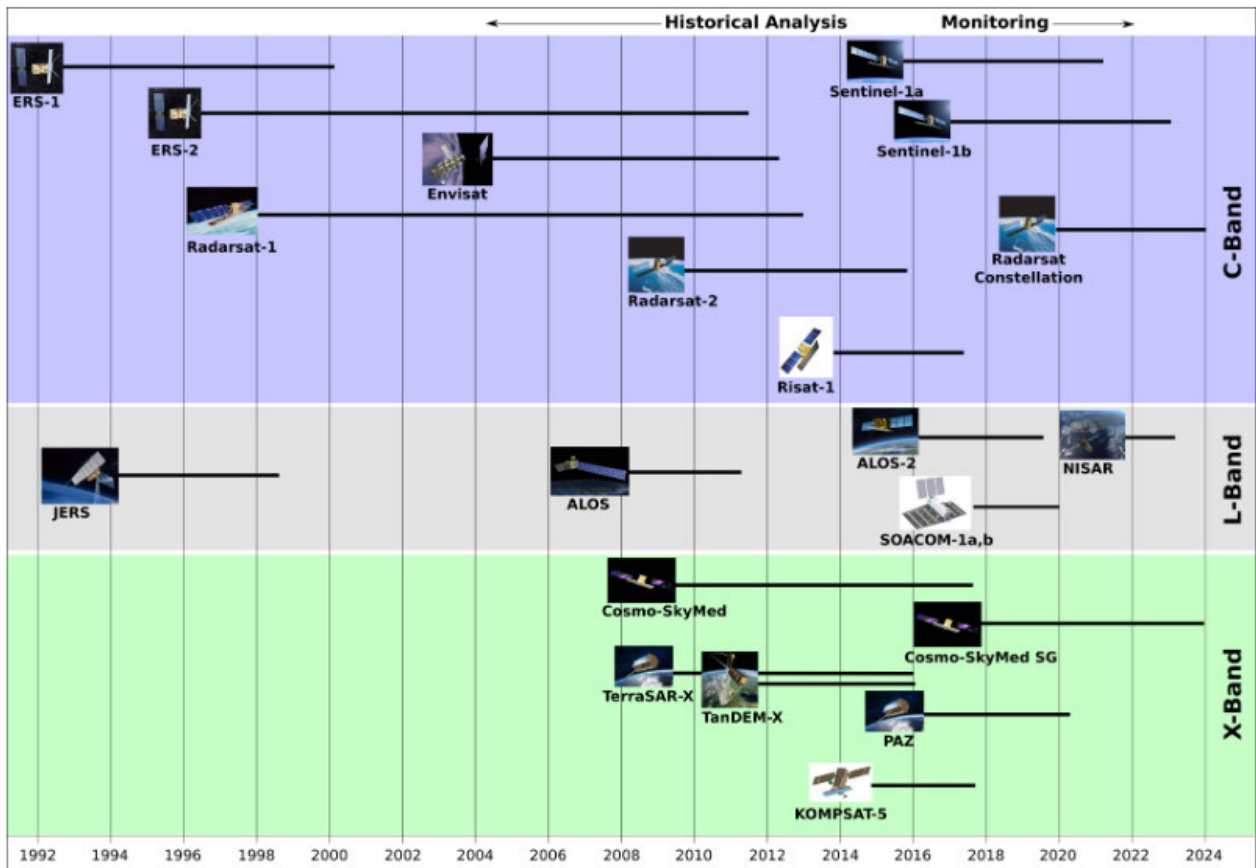


Figure 2 Outline of SAR Satellite Missions (UNAVCO, 2018)

As this project aims to use the data provided by the Sentinel 1 mission a brief overview of this mission will be undertaken. The sentinel 1 mission is one of many used as part of the broader Copernicus earth observation programme. This mission consists of several satellites that will be brought into operation overtime, the first is known as Sentinel-1A launched on 3 April 2014 followed by Sentinel-1B launched which was launched on 25 April 2016. An important feature is the repeat observation times of 12 days per satellite or 6 days where both satellites make observations, Yague-Martinez et al. (2016) report this is significantly reduced compared to the ERS-1, ERS-2, and Envisat which were 35 days between observations. One advanced feature that is of interest is the ability of the satellite due to onboard instruments is to provide detailed orbit information.

Sentinel 1 missions use C-band SAR instruments with four imaging types the main two are Interferometric Wide-swath mode (IW) Wave mode (WV) it also uses Strip Map mode (SM) and Extra Wide-swath mode (EW). The main mode is IW for imaging of stable surfaces. A depiction of these modes is shown in Figure 3 below.

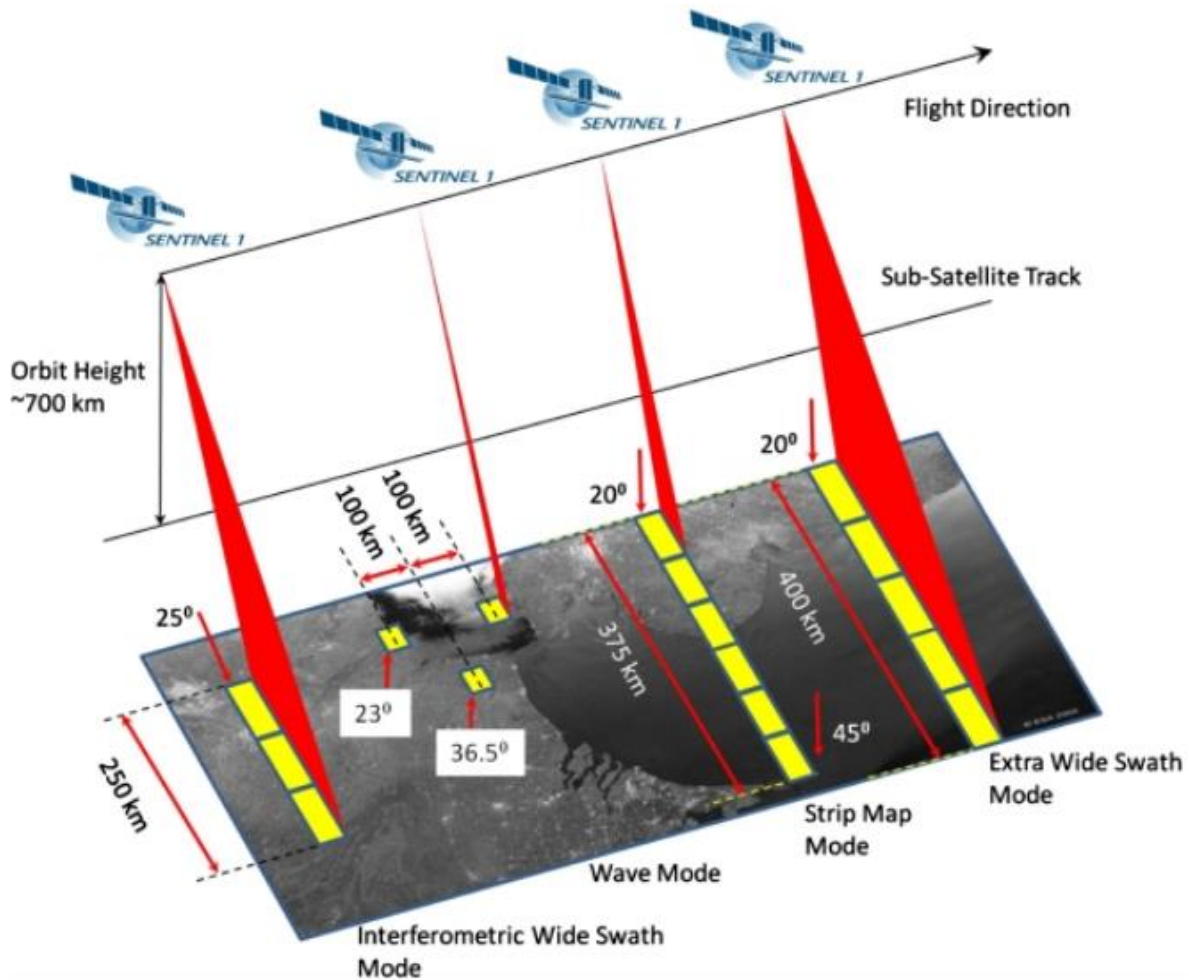


Figure 3 Sentinel 1 Image acquisition modes (European Space Agency, 2012)

The IW mode, through the utilisation of Terrain Observation by Progressive Scans also known as TOPSAR, allows for large swath width of 250 km while still maintaining high resolution with 5x20 m ground pixels (European Space Agency, 2012). TOPSAR allows this as explained by Yague-Martinez et al. (2016), in Figure 4 below shows the electronic steering of the beam in the azimuth direction which starts with the IW1 (Blue) once complete moves to IW2 (Green) and once complete moves to IW3 (Red). This allows for three subswaths to be generated for each burst which is the echo recorded. Another benefit of using this method is it reduces scalloping as reported by Yague-Martinez et al. (2016).

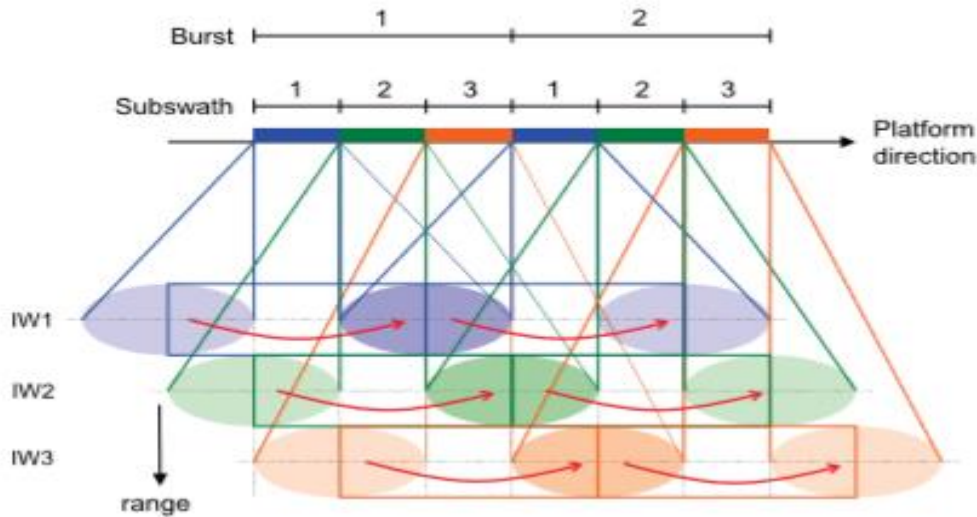


Figure 4 IW TOPSAR scan pattern (Yague-Martinez et. al, 2016)

Sentinel 1 data produces a range of products for varying number of uses. These include single look complex (SLC) used for interferometry, Ground Range Detected (GRD) products for when only the amplitude is required and an ocean product for wind, wave and current applications (European Space Agency, 2012).

The European Space Agency refers to the SLC data contains both amplitude and the phase component, which is preserved using full available bandwidth and both real and imaginary components. The product has been corrected for satellite errors including being geo-referenced using satellite geometry and orbit information, the data is provided in line of sight range observation coordinate. The GRD product is one which has already undergone some processing by being multi-looked and projected the slant range to ground range using in this case Earth ellipsoid model WGS84 (European Space Agency, 2012). This processing results in complete loss of phase therefore, the resultant pixels only relate to amplitude. This makes the GRD product ineffective for interferometry applications.

2.2.3 Radar Polarisation

Polarisation refers to the specific orientation or plane the emitted wave oscillates towards the target. That is for EM waves perpendicular to the direction in which they are propagated, for SAR sensors these can be either horizontal or vertical planes. Horizontal polarisation is when the wave is perpendicular to the plane of incidence, Vertical is perpendicular to both the horizontal polarisation and propagation direction. Therefore, it is corresponding to the plane of incidence as described by Van Zyl J & Kim Y (2011). The sentinel 1 satellites SAR sensor operates in the either single HH and VV polarisation or dual polarisation HH and HV or VV and VH. Where the first letter is the emitted polarisation and the second the received polarisation (European Space Agency, 2012).

A study into polarization diversity in radars by Giuli (1966) points out that the returned signal may only be partially polarised due to variation in the polarisation of the returned signal. These effects can be a result of moving targets in the image such as vegetation. A further and more recent study into the effects of polarisation on DInSAR results by Schneider & Papathanassiou (2007) concluded that while these can cause errors in the results it is not of significance factor in DInSAR results.

2.3 Interferometric Synthetic Aperture Radar

2.3.1 Image Selection

The selection of the images used will be important to the processing described in the following section and therefore, can also influence results. Depending on the intended application the selection criteria will differ between those for DEM generation and those for monitoring movement.

Interaction between the local topography and that of the signal in each image acquired cause geomatic distortion in the image. There are three situations in which the topography effects the SAR image, the first is foreshortening, the second is layover and the third being shadowing. Foreshortening occurs when the face of the terrain increases from the horizontal plane towards the satellite, this causes an increase in amplitude but are imaged in a lower resolution than flat areas. Layover occurs when the top of slope is imaged before the bottom, and the results impose on other imaged areas. Shadowing occurs when the terrain decreases from the horizontal resulting in no image for that side as the radar operates in a side looking system (Ferretti et al, 2007). These effects are represented in the figure below.

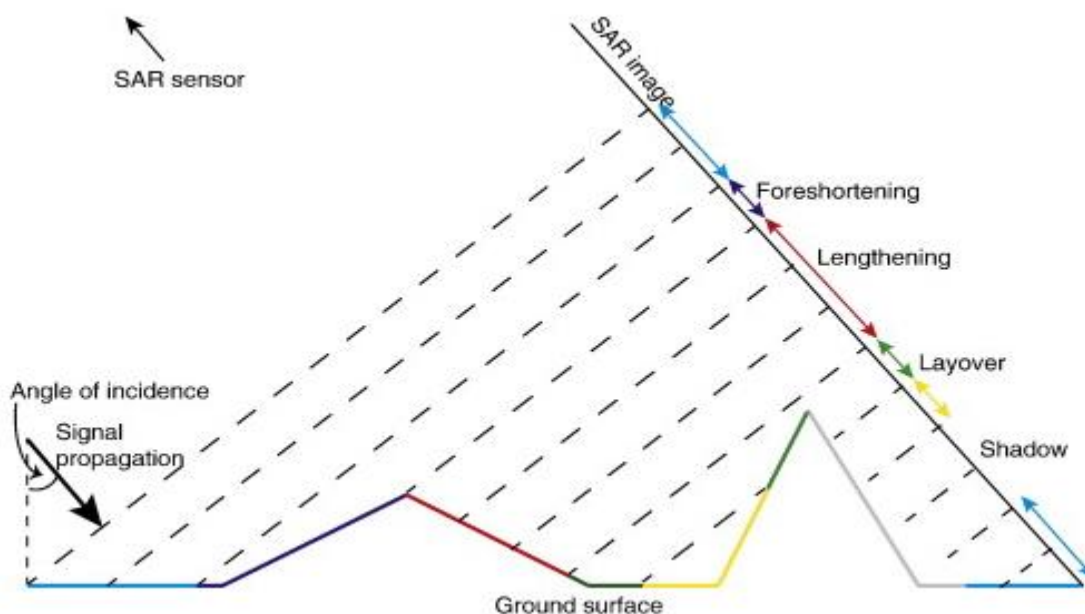


Figure 5 Effects of topography on SAR signal (Pinel, poland & Hooper, 2014)

Ferretti et al (2007) outlines some criteria to use for when selecting images for DInSAR applications, these include the following;

- Select images that avoid foreshortening or layover by using either ascending or descending images.
- The smaller the perpendicular baseline used the less effect topography has on the result therefore, the resulting movement is more accurate. It also means a less precise DEM will be required in the process.
- Coherence in the images is affected by forested areas and water basins lose coherence after 1 day. Like those mentioned areas of agriculture crop production will have high coherence but losses it relatively quickly being around 35 days from first imaging.
- However, urban areas or those with exposed stable features such as rock will maintain high level of coherence over a long time period.

2.3.2 InSAR Processing

Interferometric Synthetic Aperture Radar (InSAR) technique refers to the creation of velocity maps for the purpose of detecting the change of the earth's surface or dielectric properties through the difference phase and multiplication of amplitude (Zhou X, Chang & Li, 2009). The interferograms are generated through the cross multiplication of the first SAR image known as the master and with the complex conjugate of the second image known as the slave (Ferretti et al, 2007).

SAR data can be collected in the form of single pass interferometry or in a repeat pass interferometry mode. The first method utilises one platform for two antennas, as a result, the time for the acquisitions is very short. Collection for this method is done using only one antenna to transmit and receive the returned signal or where two antennas are used to both transmit and receive, this is also known as ping-pong mode (Fielding N.D). For repeat pass interferometry the images are taken from a closely aligned geometrical point, but they are separated by a time difference from days to years (Zhou X, Chang & Li, 2009).

This relationship of time and imaging location in the acquisition can determine whether the phase difference is related to topography or ground deformation. Ge, Chang & Rizos (2007) state that if the same time but different sensor location is used the phase difference relates to topography, whilst using the same sensor location with time differencing results in phase change due to deformation. However, with repeat pass interferometry the area will be imaged at both different times and slightly different locations due to the orbit of the satellites therefore containing both topography and deformation as components of the phase.

There are many steps that need to be followed in order to generate meaningful results. The first being coregistration which is achieved by aligning the pixels of the slave image to that of the master images which are to be used. This ensures that the pixel of each image is relating to the same ground area in each image. Ferretti et al (2007) outlines that the coregistration should also account for;

- Orbit crossings/skewing's
- Different sensor attitudes
- Different sampling rates

Along and across track shifts

The interferogram generated after coregistration of the images can be described as the summation of all components effecting the phase; $\Delta \varphi_{\text{interferogram}} = \Delta \varphi_{\text{flat}} + \Delta \varphi_{\text{topography}} + \Delta \varphi_{\text{displacement}} + \Delta \varphi_{\text{orbit}} + \Delta \varphi_{\text{atmospher}} + \Delta \varphi_{\text{noise}}$. The parts of the equation can be represented in a mathematical approach, these are best described by Ferretti et al. (2007) the flattening component shown in equation 1 below.

$$\text{Eq (1)} \quad \varphi_{\text{flat}} = \frac{4\pi}{\lambda} * \frac{B_{\perp} S}{R \tan \theta}$$

Where B_{\perp} is the perpendicular baseline, s is the phase variation due to slant range displacement of the targets, λ is the transmitted wave length, R is the slant range or Line of Site (LOS) distance that is the distance between the target and satellite, θ is the incidence angle which is the angle between the target and a line perpendicular to the surface at the target.

This equation is simplified by Osmanoglu et. al. (2015) and Zhou X, Chang & Li (2009), to

$$\text{Eq (2)} \quad \varphi_{\text{flat}} = \frac{4\pi}{\lambda} * B_{\parallel}$$

Where λ is the transmitted wavelength, B_{\parallel} is the parallel baseline.

The base line information is obtained from the precise orbit information provided by ESA when undertaking InSAR using Sentinel satellites, the orbit information becomes available approximately 20 days after acquisition. Therefore, any error in the orbit information will cause error in the baseline length and thus phase change, this error is left to be known as φ_{orbit} . The flattening is the error due to the earth's curvature, as the satellite image is taken with the assumption of the earth being flat. Hence the above equation resolves the phase difference between flat and actual earth (Osmanoglu et. al.2015) this is known as interferogram flattening.

The phase difference due to the topography is the next component in the interferogram as shown by equation 3 below.

$$\text{Eq (3)} \quad \varphi_{\text{topo}} = \frac{4\pi}{\lambda} * \frac{B_n q}{R \sin \theta},$$

where q is the change in altitude between the targets, referred to a horizontal reference frame Ferretti et. al. (2007). Or as described by Zhou X, Chang & Li (2009) as the height of the pixel above a horizontal reference frame. The removal of this component will be discussed further in the following section as this is what becomes known as Differential InSAR (DInSAR).

Where a change occurs during the acquisition times, it is represented in the equation as the term $\varphi_{\text{displacement}}$. Ferretti et. al. (2007) states the term is independent of baselines and described mathematically by equation 4.

$$\text{Eq (4)} \quad \frac{4\pi}{\lambda} * d,$$

Where d is equal to the change in range distance between the imaging times.

The remaining terms $\Delta_{\text{atmosphere}}$ is the delay in the travel of the radar signal caused by atmospheric effects from both the ionosphere and troposphere, these could be modelled using local GPS networks such as CORS network Ge, Chang & Rizos, (2007). Another option to account for atmosphere delay is to stack multiple interferograms and use stable targets in the images to identify the portion of phase change these effects have caused and thus use that value to remove that portion of change from the image (Zhou X, Chang & Li, 2009). Finally, Δ_{noise} , which is the remaining noise encountered, this term is estimated in the form of coherence and is discussed further below. Depending on the intended purpose, it is these above components that need to be removed to isolate the desired effect to remain such as topography for DEM creation or displacement for deformation monitoring (Ge, Chang & Rizos, 2007).

As identified from the information above the interferogram can be represented by the following equation,

$$\text{Eq (5)} \quad \Delta\varphi = \frac{4\pi}{\lambda} * B_{\parallel} + \frac{4\pi}{\lambda} * \frac{B_n q}{R \sin \theta} + \frac{4\pi}{\lambda} * d + \Delta\varphi_{\text{atmosphere}} + \Delta\varphi_{\text{noise}}$$

The coherence between the images is required to show the similarities between the pixels in two images and therefore, provides an indication as to the quality of the interferogram. Osmanoglu et. al. (2015) and Ferretti et. al. (2007) have identified the following components that effect the correlation, these components are multiplied to obtain the total coherence value for the pixels. The first is γ_{temporal} this the effect caused by the time difference between acquisitions, the second is γ_{doppler} which the effect of any attitude (yaw, roll & pitch) differences of the satellite between the master and slave images, γ_{baseline} this induced through separation of the satellites orbits and finally $\gamma_{\text{volumetric}}$ this caused by vegetation as such it cannot be avoided. Coherence of an area is represented by the following equation

$$\text{Eq (6)} \quad \gamma = \gamma_{\text{temporal}} * \gamma_{\text{doppler}} * \gamma_{\text{baseline}} * \gamma_{\text{volumetric}}$$

The values for coherence are represented by values between 1 and 0, where 1 represents areas of full coherence and 0 representing areas of complete loss of coherence. Areas that have good coherence are those that have stable features such as urban areas, and those that have little to no coherence are areas that contain vegetation or bodies of water. On the coherence map the brighter the pixel, the greater the coherence and hence dark pixels represent areas of poor coherence. A coherence value of 0.5 to 1 is considered to display accurate deformation rates, and less than 0.5 is considered to produce poor results (McClusky & Tregoning, 2013).

2.3.3 Differential InSAR

DInSAR refers to the specifically to the interferogram whereby the topography component has been removed, this will result in a phase difference from deformation only, an example of DInSAR is below in Figure 6. The removal of the topographic component is done by three ways as described by Ferretti et al (2007), with the first is using a single interferometric pair of images with a near-zero baseline and therefore, topography has no effect. The second is via a digital elevation model when a single interferometric pair is used with a non near-zero baseline. The third option is to use three pass interferometry where two images contain no motion. However, this paper will use the DEM method to remove this component.

The selection of the Digital Elevation Model (DEM) is to be of a quality that does not negatively affect the DInSAR results, the higher quality of DEM used the smaller the residuals in the topographic signal (Ge, Chang & Rizos, 2007). The three arc second DEM available from the Shuttle Radar Terrain Model (SRTM) has been reported to be of sufficient accuracy and also the added advantage of worldwide coverage with the exception of the polar areas (McClusky & Tregoning, 2013).

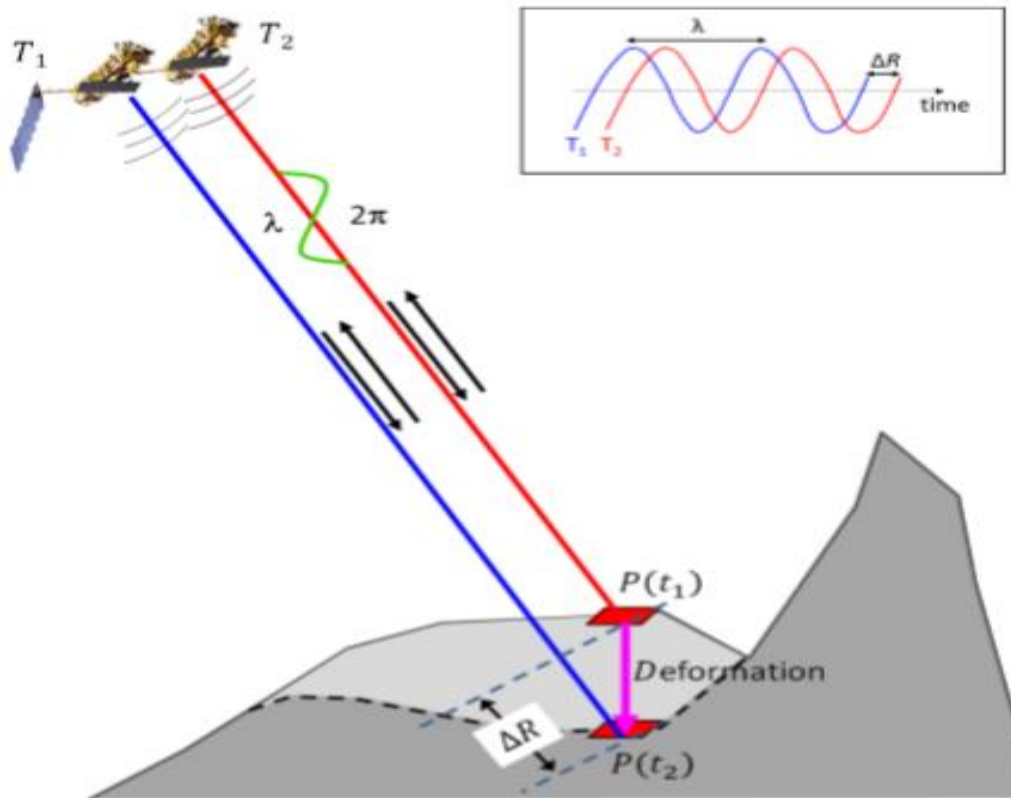


Figure 6 Example of basic DInSAR (Sousa & Bastos, 2013)

This is the first and most widely researched deformation technique on which many of the more advanced time series techniques are based. These include Persistent Scatter Interferometry (PSI) is an advanced DInSAR technique requiring the identification of stable features in the scene in order to establish and remove atmospheric effects however a study by Guoqing & Jingqin (2008) suggest that this technique would require at least 20 images and a close to linear deformation type. This project will use the DInSAR technique, and the following studies which are revised are based upon this technique.

2.3.4 Phase Unwrapping

As the phase of the SAR data is a sinusoidal wave that is constrained between $-\pi$ and π , the interferogram is known as wrapped. In the wrapped stage where there is a discontinuity in the cycle, the map shows these as fringes, which are represented by a change of colour which is arbitrary to the result. These fringes equate to half the wavelength; therefore, the fringes can be counted and multiplied by half the wavelength. For example, one fringe of C-Band which has a wavelength is 5.6cm so the deformation would equal 2.8cm.

To make use of the produced velocity map, it then requires that the interferogram is unwrapped to display the continuous change. The unwrapping of the phase is described by Veci (2016), as to solve ‘the ambiguity of altitude by integrating phase difference in neighbouring pixels, then deleting any

integer number of altitude ambiguity equivalent to the 2π cycle'. After this, the unwrapped image shows the continuous phase change and reveal the actual change between the pixels.

The altitude of ambiguity is defined by Ferretti et al. (2007) as 'the altitude difference that generates a phase change of 2π after flattening the interferogram', it is expressed by

$$\text{Eq (7)} \quad h_a = \frac{\lambda * R \sin(\theta)}{2B_n}.$$

The noise in the interferogram can affect the quality of the unwrapped result, Veci (2016) states it may be necessary to increase the noise to signal ratio by applying filtering.

2.3.5 Noise Filtering

The removal of the noise completely is not possible however, there are filters which can be used to reduce noise and increase the signal to noise ratio and enhance the unwrapping. There are two common filters which are applied to the compiled interferogram, these are complex multi-looking and Goldstein phase filtering.

Complex multi-looking filtering reduces noise through spatial averaging data over a number of neighbouring pixels, this form of filtering is effective for time, baseline and vegetation induced noise, but cannot remove space related noise such as atmosphere. Whilst an effective method it does, however, reduce the spatial resolution (Ferretti et al, 2007). Pepe and Calo (2017) also agree that it is an effective method for phase filtering and reduces spatial resolution. They also state this loss of spatial resolution does not have a drastic effect on the results.

The Goldstein filter was introduced by Goldstein and Werner (1998) for the application of improving measurement and phase unwrapping accuracies. This filter is described by Goldstein and Werner (1998) as smoothing the intensity of Fourier transformed overlapping segments of the interferogram. The adaptive nature of this filter means that areas of low coherence are weakly filtered and those with high coherence are filtered strongly, therefore increasing the fringe visibility.

2.4 Applications of InSAR

The use of InSAR technique is suited to a variety of applications whereby there is a detectable change in the land surface of an area over a period of time. Having the ability to easily and economically detect these changes, it has made this remote sensing technique appealing to many fields of research.

2.4.1 Geomorphology

Geomorphology is one such field where there are many real-world applications for using InSAR. These include land subsidence monitoring and detection in urban areas and areas around activities such as resource extraction of coal, gas and ground water. Other geomorphology areas where InSAR is applicable for use is in the study of seismic activity/events for monitoring the land surrounding faults, volcanic activity to monitor the area before and after eruption, landslides, sand dune movement as reported by Maghsoodi et.al. (2013), Zhou X, Chang & Li (2009) and Smith (2002) in their respective studies into the applications of InSAR.

2.4.2 Hydrology

The hydrology takes advantage of the amplitude component of the waves used as opposed to the phase length as used in other applications. Both Zhou X, Chang & Li (2009) and Smith (2002) also indicate in their studies of InSAR applications that hydrology is another area in which this technique can be applied. These include the soil moisture monitoring, snow/glacier monitoring, water level in rivers, dams, and urban areas during floods.

2.4.3 Infrastructure monitoring

Whilst the above outlines the more common areas in which InSAR has been used, there are some more emerging areas of research, such as in the monitoring of assets like dams, bridges, and roads. A recent study (Zhou W et al.,2016) on the settlement monitoring of Shuibuya Dam in China, has shown the effectiveness of InSAR in this situation. During the study, they used 21 images obtained from February 2007 to March 2011, from this they found the results to have good correlation when compared to the results from the traditional methods. Another advantage noted from this study is that through the application of InSAR the surrounding area of the dam can also be monitored at this same time as opposed to the traditional methods used.

2.5 Land Movement Detection

2.5.1 Traditional Techniques

The detection, mapping, and monitoring land movement has historically relied upon terrestrial based techniques. These include firstly the use of the precision optical or digital level, in more recent times GNSS has been utilised and in some cases the use of a total station, the method used would depend on the accuracy required. The methods are similar in that the movement is related to designated points at set locations where benchmarks are placed to ensure the consistent site is used throughout the time

period. Sabunchu and Ozner (2013) recognise that precision levelling is the most precise technique amongst all the techniques, however using GNSS has provided a saving in time as it requires less people but has a higher cost for instruments than levelling.

Whilst the traditional techniques provide data with a better temporal resolution than SAR, however due to the point to point nature does not provide a high spatial resolution compared to InSAR, and hence a better description of the subsidence that is or has occurred is obtained through the (Yang & Peng, 2014).

2.5.2 DInSAR Studies

The use of DInSAR for detection of land movement has progressed since its time of inception with the expansion of the number of systems acquiring the data. This technique is becoming more accepted throughout the world and has been used in many studies for various land movement detection and monitoring applications. This section will provide a background as to what has been achieved in previous studies from throughout the world and in Australia.

Hangdong et al. (2011) conducted a study into the subsidence events in the Jiangsu province in China. The study used data from ERS 1/2 captured six scenes from the period of July 1995 to May 2000, this resulted in the creation of three interferograms from three time periods with twelve to nineteen months between images. Using DInSAR technique subsidence results were obtained for all scenes; however, ground data comparison was only made for the period from October 1998 to May 2005. They found subsidence to range from -10mm to -30mm over the area. In the last time period an analysis of the results found an up lift of 10 mm to the north and a subsidence of less than -30mm in the south, however, due to the long time period between acquisition it could not be determined whether this is caused by an error in processing such as unwrapping, atmospheric error or due to changes in wet and dry seasons. If a shorter time period between images were used a determination of the results in the last period could have been better determination as to the cause of the results. Finally, it was determined that the DInSAR technique is suitable for this application and found a linear relationship to subsidence velocity and water extraction is identifiable.

A study conducted by Chatterjee et al. (2015) aimed to detect, map, and monitor subsidence in the Jharia coalfield in Jharkhand, India. They aimed to do this by multiband DInSAR with validation through comparison with precision levelling and GPS. The InSAR data was collected from ENVISAT ASAR in C-band with an observation period of 2003-2004 and 2007, and ALOS PALSAR in L-band acquired during 2007-2008 with six pairs of each used. However, the overlap of terrestrial data and satellite data was only a relatively short time frame of 5 months for the C-band and 14 months for L-band. Despite this the study concluded that the subsidence rate has a strong correlation between all techniques and suggests that InSAR technique is suitable for this purpose.

These local studies have been for the purpose of monitoring the areas surrounding mining activities of both coal and coal seam gas.

Ng et al. (2010) conducted a study over the coal fields in New South Wales Sydney basin; it found that the variance in results ranged from 0 to 48 mm with an average of 12mm when compared with GPS data. Which showed that the results are still useful in monitoring subsidence from DInSAR even though they had limited data and only studied a relatively short time frame which only had 10 images captured over fifteen months. The study had aimed to use Persistent Scatter InSAR or PSInSAR to remove the atmospheric effects and obtain mm accuracy. However, due to the location, it lacked coherent targets. Also, a condition of this technique is the need for a minimum of 20 images to make use of PSInSAR (Guoqing & Jingquin, 2008), but only 10 images were used in this study.

Parker et al. (2015) conducted a study over the Perth basin using both Sentinel-1A and TerraSAR-X satellites. However, due to the limited availability of images in the area from Sentinel-1A, it was only a short seven-month comparison for the two satellites. The study used a longer imaging time for the TerraSAR-X, which proved that the satellites have good coherence in results, therefore demonstrating the ability of the Sentinel satellite data to be useful in subsidence monitoring. While it shows the satellites are of similar ability, it did not prove due to lack of data whether the subsidence is due to long term subsidence or natural fluctuations in the ground from the hydrological cycle. An extended period of study would be required for this determination.

The other studies specific to Australia including (Ge et al., 2007, & Ng et al., 2014) have all agreed that DInSAR can achieve results that have good coherence with traditional survey technique results in relation to subsidence monitoring over mining areas. Whilst these studies have proved the effectiveness of the technique there is little study into subsidence in disused mine sites which have been redeveloped to housing.

2.6 Conclusion

The literature review of previous studies has shown the results from this method can be expected to have good consistency with those of traditional techniques. It has also identified some key criteria that need to be considered throughout the project. This being to ensure meaningful results that consideration is given when selecting the site so that coherence can be maintained, i.e. construction works or vegetation etc. that could give false positive deformation change, the DEM selected is of a suitable nature to remove the topography phase. The images also need to be from the same orbit track

in order to obtain the deformation result. The baseline can influence the results as well as the need to filter the interferogram prior to unwrapping.

3 Methodology

3.1 Introduction

This chapter is intended to aid the readers understanding of the project’s development through outlining the methodology to meet the projects aims and objectives. The methodology was created using the literature review to guide the processing and provide the requirements to gain meaningful results. It starts with the data capture and selection with respect to conditions discussed in chapter 2, before moving on to the processing parameters used in the SNAP software.

3.2 Data Acquisition and Image Selection

The data for the project is freely available and was acquired from ESA through the Alaskan Satellite Facility (ASF). Initially, only six data sets were acquired starting from the first available being 15-11-2016. This was due to the processing time required and amount of data generated through processing, by doing so it allowed a quicker processing time to ascertain whether significant movement was occurring over the desired site. As can be seen in Figure 7 below the user can select their area of interest and apply appropriate filters to obtain the required data.

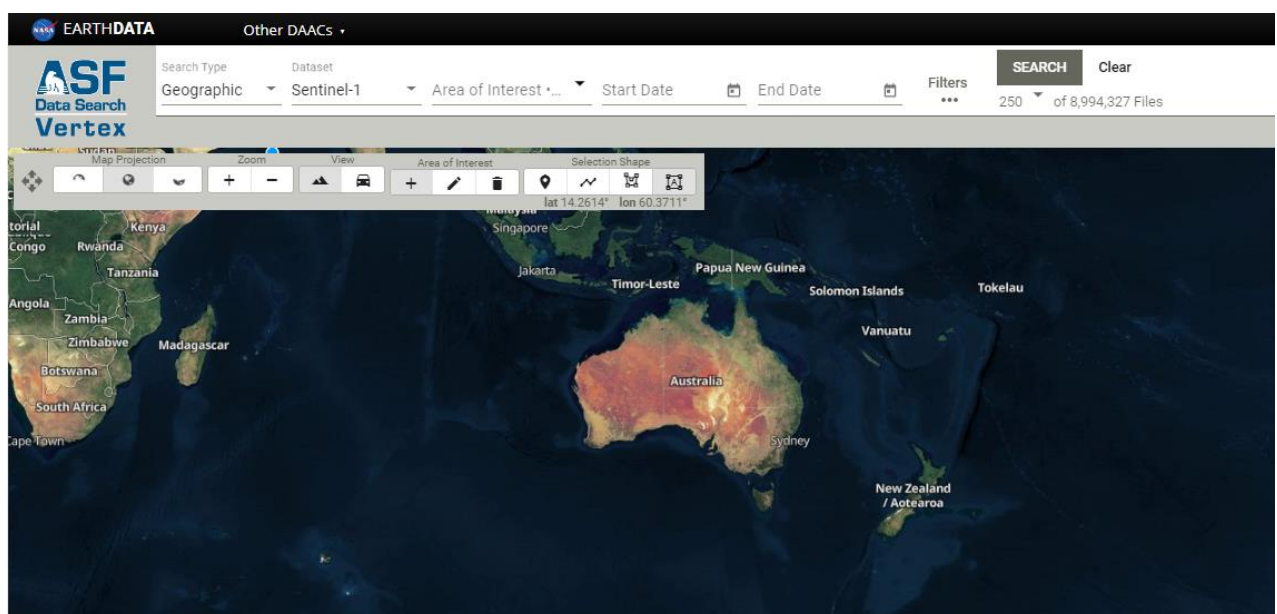


Figure 7 Alaskan Satellite Facility - search parameters (ASF, 2019)

It is important that the scenes are imaged using the same orbit path and frame otherwise the interferogram cannot be generated. Another important factor is the baselines as noted from the literature review this can influence the results. It was therefore decided, that due to number of available scenes

that path 147 and frame 681 would be used for the entirety of the project. The data is required to be in the form of a Single Look Complex (SLC) in the IW mode as discussed in chapter 2. The master and slave selection for the processing was obtained using the InSAR stack overview tool, this tool provides an overview and determines the optimal master image for processing the obtained images.

The images with the coherence above 0.5 were used as outlined in the literature review these images will produce the most meaningful results, compared to those below 0.5. This initial group will be utilised to create a series of interferograms throughout time over the area of interest.

Once these sets were completed further data was obtained and used during time periods which indicated movement. This was done to provide a reduction in the temporal base lines and therefore increase coherence and produce more results to gain better averages over the area. It also allowed for better identification as whether it was a slow subtle movement or more sudden change in the surface.

3.3 Processing

The processing of the images can be undertaken in several individual steps, or through batch processing by which the user makes a graph of the steps. However, for this project it was suitable to use the functions already set in the SNAP software using the pre-existing graphs and conducted by the following process.

3.3.1 Coregistration

The first step and one of the most important processes is the coregistration of the images. The purpose of coregistration is to align the pixels in the slave image to those in the master image to allow for proper comparison of the pixels between the two images, if not done correctly the pixels of each image will relate to different ground pixels. As previously discussed, the images of Sentinel 1 satellites are obtained using the TOPSAR data capture technique, the coregistration must be performed using the S1 TOPS Coregistration function available in SNAP.

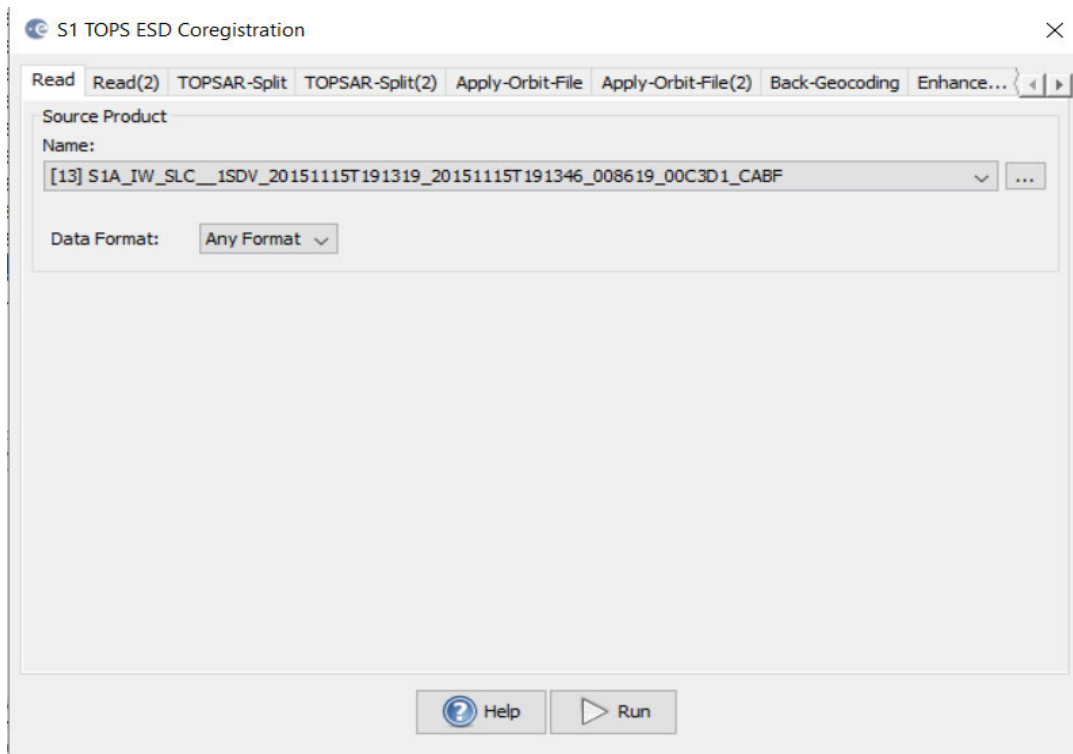


Figure 8 S1 TOPS Coregistration overview

As the images are obtained with three subswaths being IW1, IW2 and IW3 with each having nine bursts within these subswaths. The first step is the TOPSAR-Split function which allows the appropriate subswath to be selected for the area of interest. For this project it is IW1 is the subswath that contains the area of interest for the project the number of bursts can also be selected, by doing so the data size is reduced and processing time is enhanced. The Sentinel 1 satellite uses combinations of horizontal and vertical waves of polarisation for the EM waves emitted and sensed. These polarisations can be selected at this point or all polarisations can be processed, as well as the number of bursts from the subswath can also be selected at this point. The effect of polarisation selection was not trailed in this project and online forums suggest they are only minimal. The same subswaths, polarisations, and bursts must be the same for both TOPSAR Split and TOPSAR Split (2) as shown in *Figure 9*. For this project it was decided to use the VV polarisation.

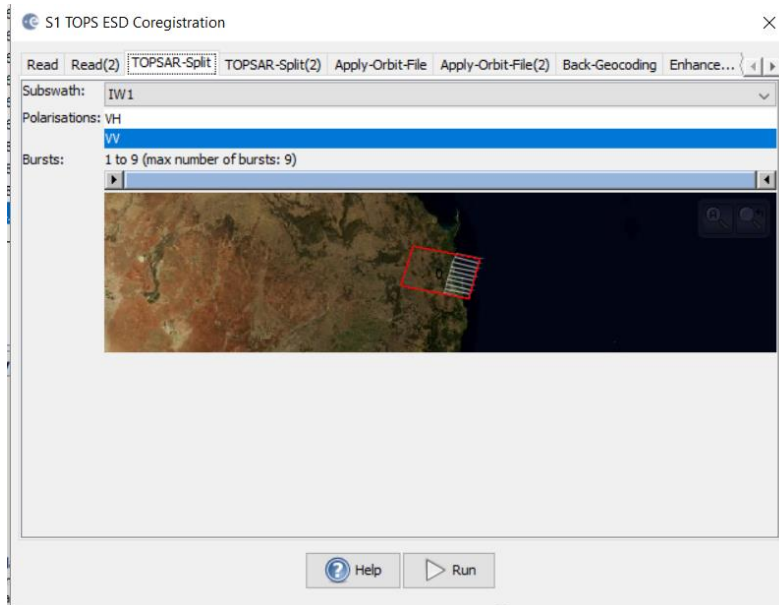


Figure 9 Subswath, polarisation & bursts selection (Master)

The orbit data for the satellites is required to compute the baselines between the image acquisition times, the metadata file of each image contains this data it is not of appropriate quality to be used in the processing. To overcome this, the Apply the orbit file function is used which provides the precise data which is made available about 20 days post acquisition as stated in chapter 2. These precise files are automatically downloaded to SNAP when using this function and automatically applied to both images.

Through the use of back geocoding the slave is resampled into the master image, there are several Digital elevation models (DEM) available for use within the SNAP software which can be set and also an option for user own DEM, the default for SNAP is the Shuttle Radar Topography Mission (STRM) 3 sec DEM. However, due to issues with the default DEM within the SNAP software at time of processing for this project, it was then decided to use the STRM 1 sec DEM is used (Figure 10). Bilinear Interpolation is used throughout the processing, as this is what is used in several tutorials.

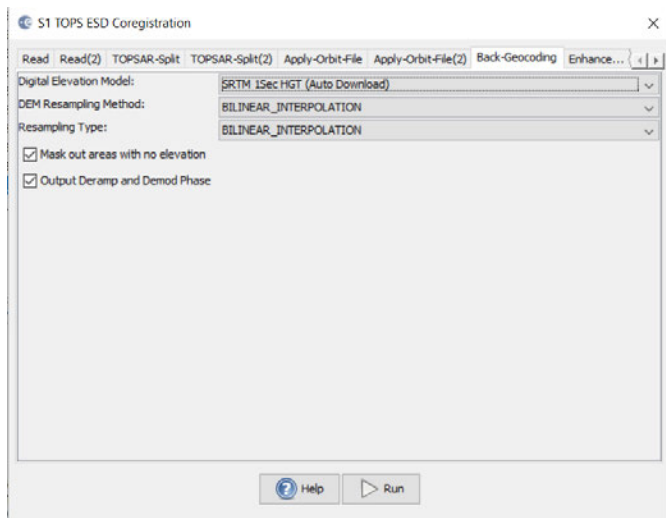


Figure 10 DEM selection for coregistration

In order to improve results of the coregistration the Enhanced Spectral Diversity (ESD) was included in the project. In the SNAP software this process allows a fine correction to the range and azimuth looks. Firstly the range offset estimate is generated using incoherent cross-correlation (ICC) technique, where patches of data at the centre of each burst to create an estimate for that burst, this is done for all bursts and finally the results are averaged to create the offset (European Space Agency, N.D).

The second step makes use of the ESD technique is used to retrieve the constant azimuth offset estimation for the image. The ESD technique exploits the data in the overlapped sections between bursts within a subswath to create the offset estimation (Prats-Iraola et al, 2012). Once this performed the offsets corrections for both range and azimuth are applied to the image. For this project the parameters used where the default parameters recommended by the product.

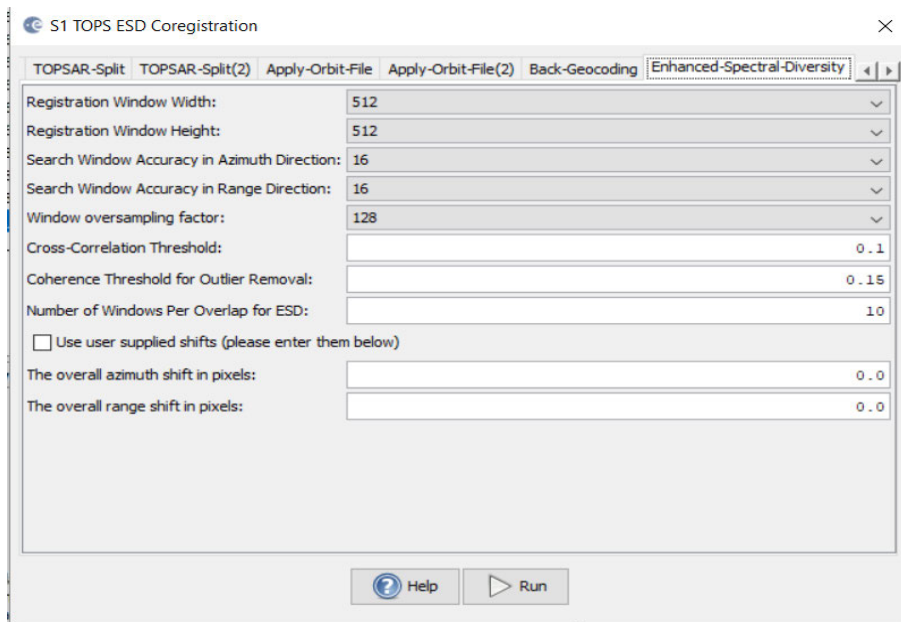


Figure 11 ESD Parameters

3.3.2 Coregistration check

Once completed a check on coregistration can be undertaken and approximate estimation of coherence can be seen by right clicking the product and select open RGB image, set the master as the red and slave as green, the change of pixel will be shown as green or red and yellow shows the area with no change and hence good coherence between images (Figure 12). If the image is shown as solid purple in colour the coregistration has failed, and the DEM selection should be investigated, as this result may indicate an issue relating to the chosen DEM.

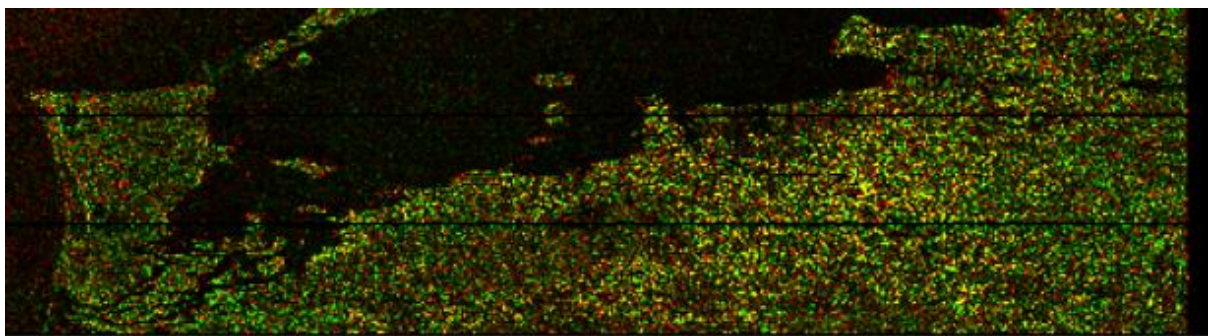


Figure 12 RGB output product

3.3.3 Interferogram Generation

The interferogram formation step is the next most important part of the processing operation, it is formed by a cross multiplication of the master and slave image. The amplitude signal of the two images is multiplied and difference the difference in phase between the two images. It is in this step that some of the unwanted phase contributions are removed, these include the flat earth component which is removed at this point and the topographic phase however, it was done further along the processing chain.

The flat earth phase as discussed in the previous chapter is the component introduced due to the curvature of the reference surface. The current reference system used for the space born SAR satellites is WGS84 (European Space Agency, N.D). Prior to removal of the flat earth phase from the interferogram it is first estimated using orbital and metadata information. This was computed over multiple points distributed throughout the entire area imaged, by using least squares to estimate 2d-polynomial to fit the observations (European Space Agency, N.D).

As shown in Figure 13 below there are several factors which were set in the parameters, for this project they were left as default. European Space Agency (N.D), state that the default value of 501 for the estimation points is sufficient for 100x100 km scenes. They also state that the 5th degree polynomial is suitable to produce smooth surface for most imaging areas around the world. These settings can be changed to suit the size of the area the imaged.

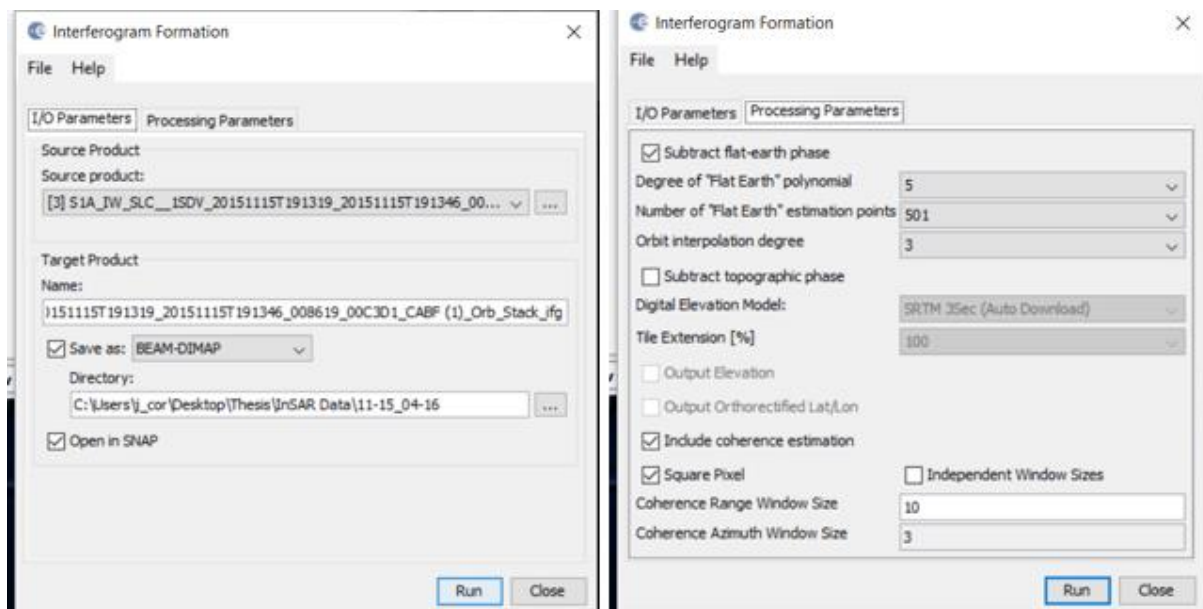


Figure 13 Interferogram processing parameters

3.3.4 TOPSAR-Deburst

With TOPSAR image capture such as that used by Sentinel 1 satellites, as discussed previously the subswaths are made up of several bursts these have a black-fill demarcation between them, this can be seen in Figure 14 below. This function removes the demarcation to make a single continuous image of the area, this must be conducted at this stage prior to any further processing.

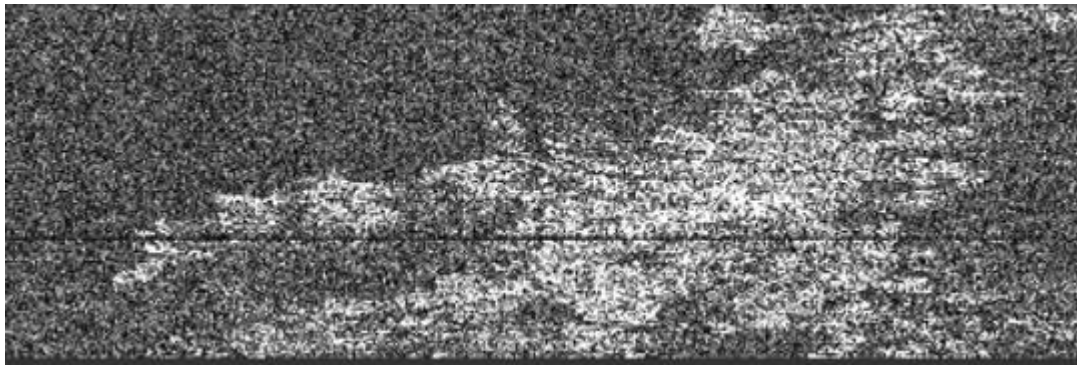


Figure 14 Example of image prior to deburst processing

3.3.5 Create Subset of the area of interest

To enhance the processing time in the following steps as the entire imaged area is not required, a subset of the image can now be created. The user is required open spatial subset and select geo-coordinates then enter coordinates for desired area (Figure 15). It is imperative that this subset product is saved before continuing to proceed with the following steps

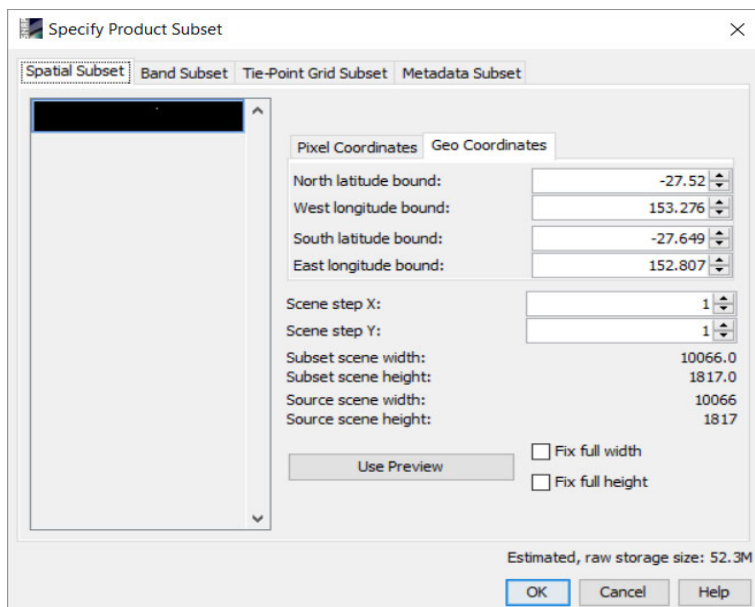


Figure 15 Geo Coordinates for area of subset

3.3.6 Topographic Phase Removal

In this step, the topographic phase component is removed from the interferogram via an external DEM which is radar coded and then subtracted from the interferogram. This is done to create a differential interferogram relating the phase change to deformation rather than the topography. In *Figure 16* below shows the parameters for the input and processing are selected, for this project the STRM 1Sec DEM has been used throughout and must be used here as well. None of the optional outputs were required for this project.

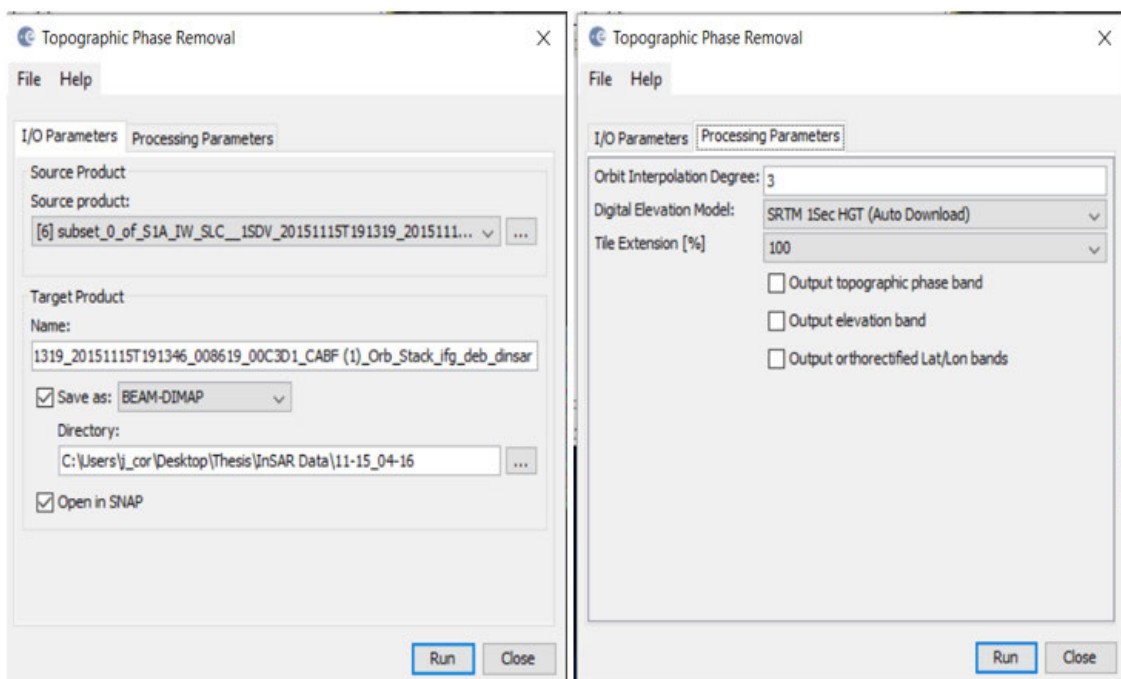


Figure 16 Topographic phase removal parameters

3.3.7 Multi-look function

The noise contained within the interferogram can be seen in the products as speckle. To reduce the inherent noise and increase the interpretability, the multi-look function was used to reduce this noise, it is computed by averaging the neighbouring pixels. It can also be used to control the pixel size, the number of pixels used can be selected for the range and azimuth. While this does reduce noise and enhance the fringe identification, it does cause a reduction in spatial resolution.

There are two input options by the user being; GR pixel where the user specifies the number of range looks and the programme determines the number of azimuth looks which results in square pixels or

independent looks where the user specifies both range and azimuth looks. For this project the GR pixel input was adopted, and parameters set as shown in the figure below.

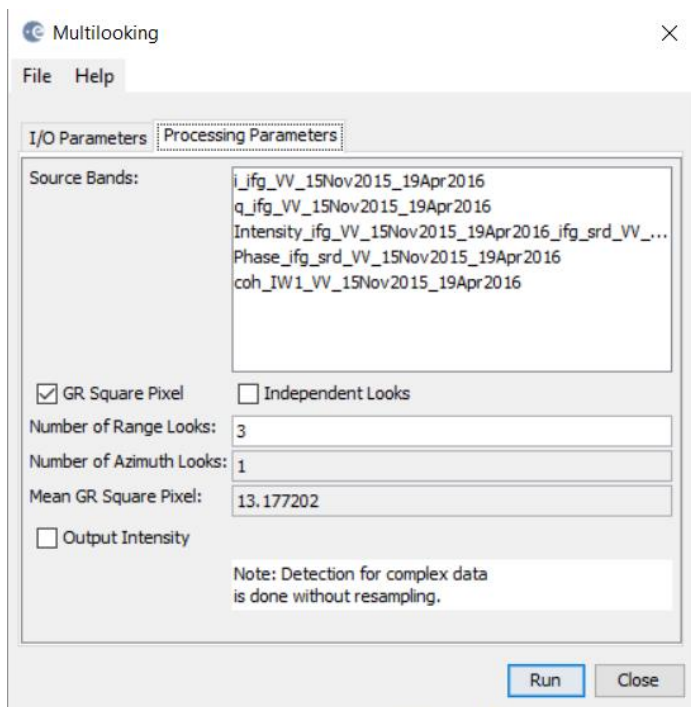


Figure 17 Multi-look Parameters

3.3.8 Goldstein Phase Filtering

As mentioned in chapter two there are many factors which contribute to the noise of an interferogram such as time, vegetation and orbit. This noise needs to be minimised to enhance phase unwrapping in the preceding steps it also minimises residuals (Goldstein & Werner, 1998) and hence the overall displacement values obtained in later processing. Therefore, it is important that this step is done prior to commencing the unwrapping. The filter applies an adaptive algorithm as such a broadband to areas of represented by low coherence usually also associated with high noise, whilst in areas where there is high coherence the narrow bandpass filtering occurs (Goldstein & Werner, 1998).

The programme allows the user to set certain parameters when using the filter operator including the adaptive filter exponent, the window size, and FFT size. The adaptive filter is set in a range from 0 to 1 whereby, 0 is no filter and 1 being full filtering with the useful value range from 0.2 to 1 (Goldstein and Warner, 1998), for this project full filtering was adopted. There is also an option to conduct coherence filtering this was set to 0.2 which is the default setting.

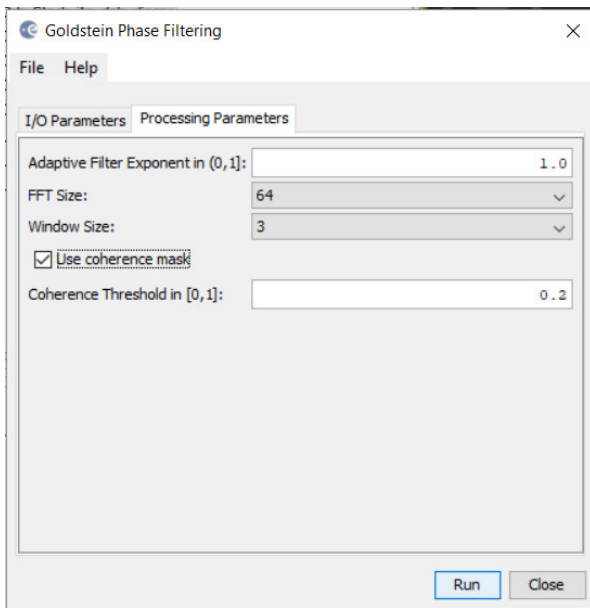


Figure 18 Goldstein Filter parameter selection

3.3.9 Phase Unwrapping

In order to solve the ambiguity of the phases and obtain a continuous change through the addition of the correct multiples of 2π . To perform the unwrapping using SNAP2U, the image must be exported in the compatible format from SNAP. A recent addition to SNAP is the SNAP2U plugin which gives the user the ability to unwrap the phase without needing to run both Linux and Windows. Through the export function the data and metadata are bundled and written to a new folder. The user then selects the appropriate parameters in this case it is DEFO, MCF with all other values left at default settings.

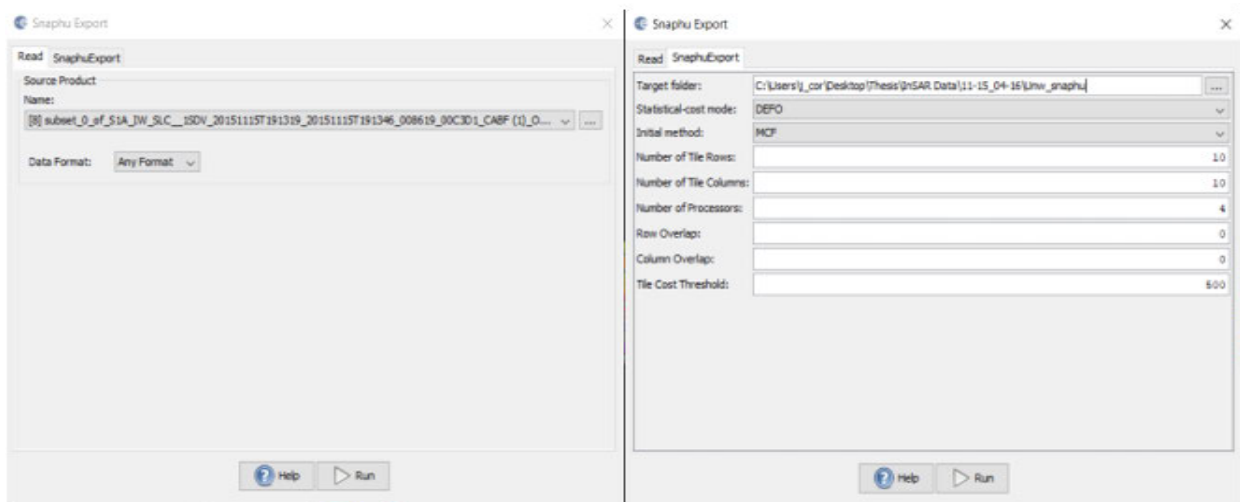


Figure 19 SNAP2U export parameters

The user can now simply undertake the phase unwrapping process by selecting the input parameters which is the done by selecting the phase.hdr file from the target location of the previous step (*Figure 20*), once these are set the program automatically computes the unwrapped phase is placed into the bundle of data exported.

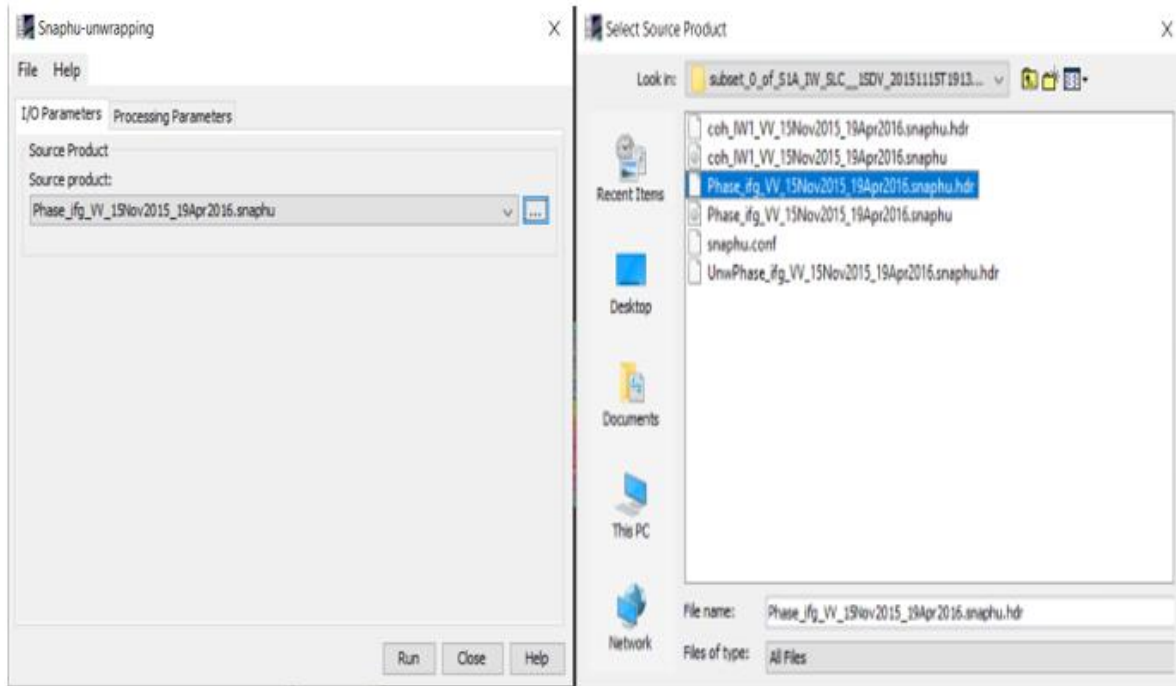


Figure 20 SNAPHU Input parameters

After the unwrapping has been executed, the product is then available to be reimported to SNAP for further processing. The user selects inputs the required parameters to be able for the re-importation of the unwrapped product. This unwrapped product is easier to interpret than the wrapped, however, further operators are used to enhance this assessment of the interferogram.

3.3.10 Phase to Displacement

Once the phase unwrapping has occurred, the interferogram image is still expressed only in phase terms of the wavelength. This operator converts the phase terms to a displacement displayed in meters; however, the expressed displacement is measured only in the line of sight direction, which is the look direction of the sensor. Therefore, meaning it does not display the true vertical movement but one that also contains a horizontal contribution. The resultant image allows for areas of movement to be more easily detected and further assessment on a pixel by pixel basis to occur.

In order to obtain the absolute movement value, the image must be tied to a point in the image where the movement is known. This could also be achieved in cases where the point has not been monitored

during the acquisition period, the user could identify stable points in the image or average the movement of several stable pixels and then subtract that value from the interferogram. Or using historical data and knowledge of the area identify stable points and subtract their obtain value from the interferogram.

3.3.11 Terrain Correction

This is the final step before exporting the data for further processing in GIS programmes or displaying results within products such as google earth. Terrain correction is the process of adjusting the image for geometric distortions, this is adjusting the image location to that of its real-world location. For this project it was chosen to use the Range-Doppler Terrain Correction tool in SNAP, other options are available within the programme to do so. Again, the STRM 1” DEM needs to be selected, individual or multiple bands can be selected for terrain correction for this project all bands where used. The BILINEAR_INTERPOLATION was again used in the process.

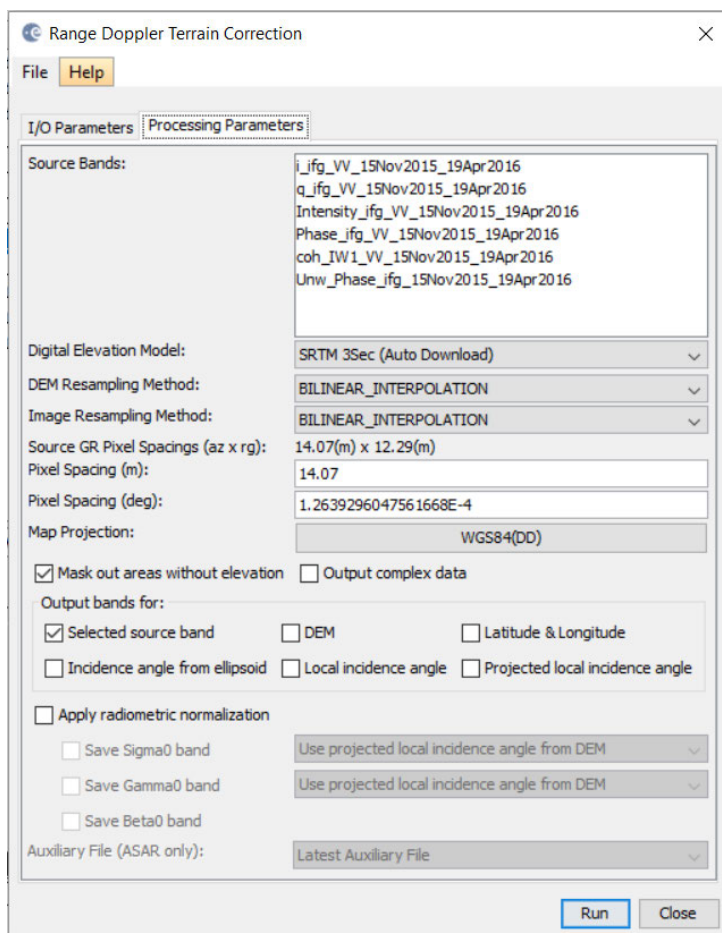


Figure 21 Terrain correction processing parameters

3.3.12 Coherence Masking

Coherence masking is used whenever the user wishes to eliminate pixels under a certain coherence, this is used in the filtering. It can be used throughout when exporting images so that only meaningful pixels are displayed. To do this the user selects the properties function on their chosen output and using valid pixel expression enters the masking requirement i.e. $\text{coh_IW1_VV_15Nov2015_29Dec2018} > 0.4$ to mask all coherence greater than 0.4. This was used in the project when displaying the final product and can be used prior to exporting areas of pixels for further analysis in products such as excel.

For this project both the unwrapped image and displacement image were terrain corrected, then stacked together. This was required to be able to undertake coherence masking on the final displacement product.

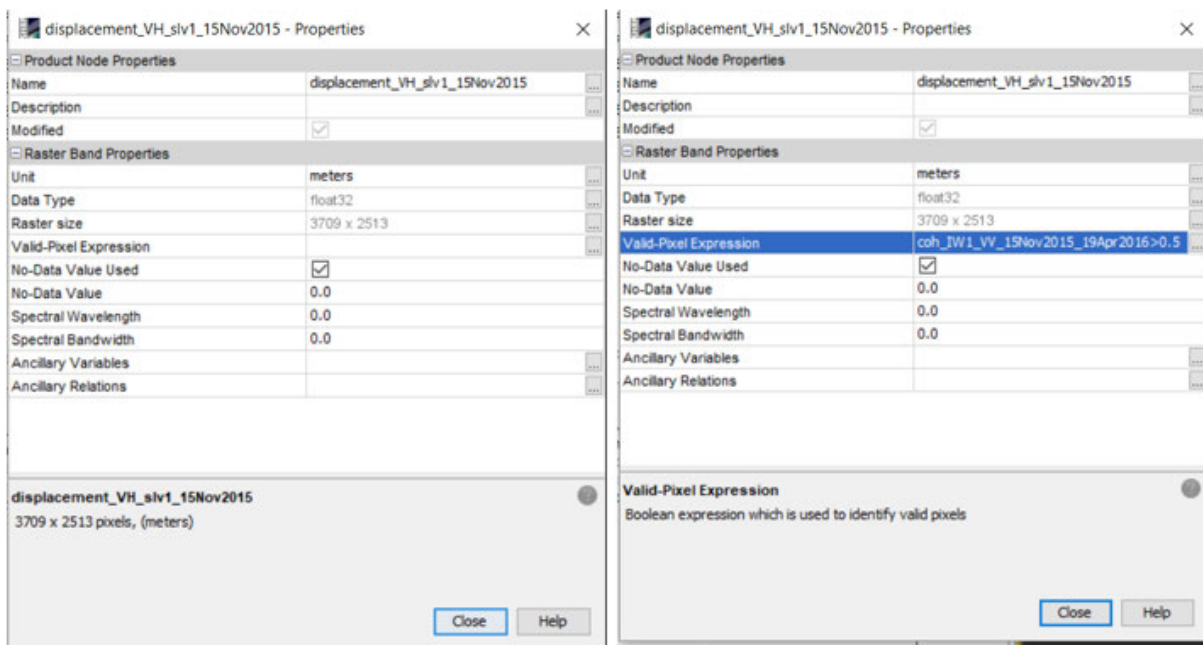


Figure 22 Coherence masking properties

3.4 Stable point identification

As mentioned above, the phase to displacement does not result in an absolute phase displacement. The absolute displacement for the area can be obtained by removing the displacement from the interferogram for a known stable point, through the use of band maths to create a new band of displacement. As mentioned in chapter 2 the identification of a stable point for a phase can also assist in the elimination of atmospheric effects. For this project it was sufficient to apply this technique, it was

done by assessing all the generated interferograms pixels through the use of excel. Once areas of high coherence were identified these points were uploaded to google earth by csv file, to assess the area for its likely hood of being stable. The displacement distance for the pixels was then averaged and applied to the interferogram.

Local knowledge in the subject area can also help in identifying points which are likely to remain stable though out the time period. This is especially important information in areas such as where this project was undertaken as no reliable continuous monitoring data was available for the area.

4 Results and Discussion

4.1 Introduction

This chapter displays and discusses the achieved results over the area of interest, a velocity map of the area was created to show that movement has occurred over each of the imaging periods used. Numerous velocity maps were created using several pairs of SAR images over a three-year period. The images used were from the following dates; 11 November 2015, 19 April 2016, 03 December 2016, 17 June 2017, 22 December 2017, 18 June 2018, 18 October 2018 & 29 December 2018. Whilst the results have been corrected for approximate absolute displacement, they should be interpreted relative to each pixel to obtain true displacement over an area, meaning the actual displacement is not the displayed value. Therefore, where any change has occurred in the area it will be shown by a varying colour in the resultant displacement image. The images were exported to excel which allowed a better understanding of the results for each time period an example is shown in Appendix B.

The figure below shows the area of interest, which is denoted by the red polygon, has been subject to mining in the past. The white area depicts area where underground mining has occurred, and the light grey is area influenced by this mining activity.



Figure 23 Mining area (Ipswich City Council, 2018)

4.2 DInSAR Results

Through investigation of all the interferograms it was decided to use an averaging of the most consistent coherence points throughout the time period. The area that maintained the best coherence over the time through all interferograms is shown in Figure 24 below. This area maintains a coherence of greater than 0.97 indicating that it is a stable phase location, which was used during the processing to estimate atmospheric effects. This site was also a good candidate as being a stable location, through local knowledge of the area it is known that during its construction significant works were undertaken to ensure the buildings stability, which provides confidence this structure is of a stable nature.

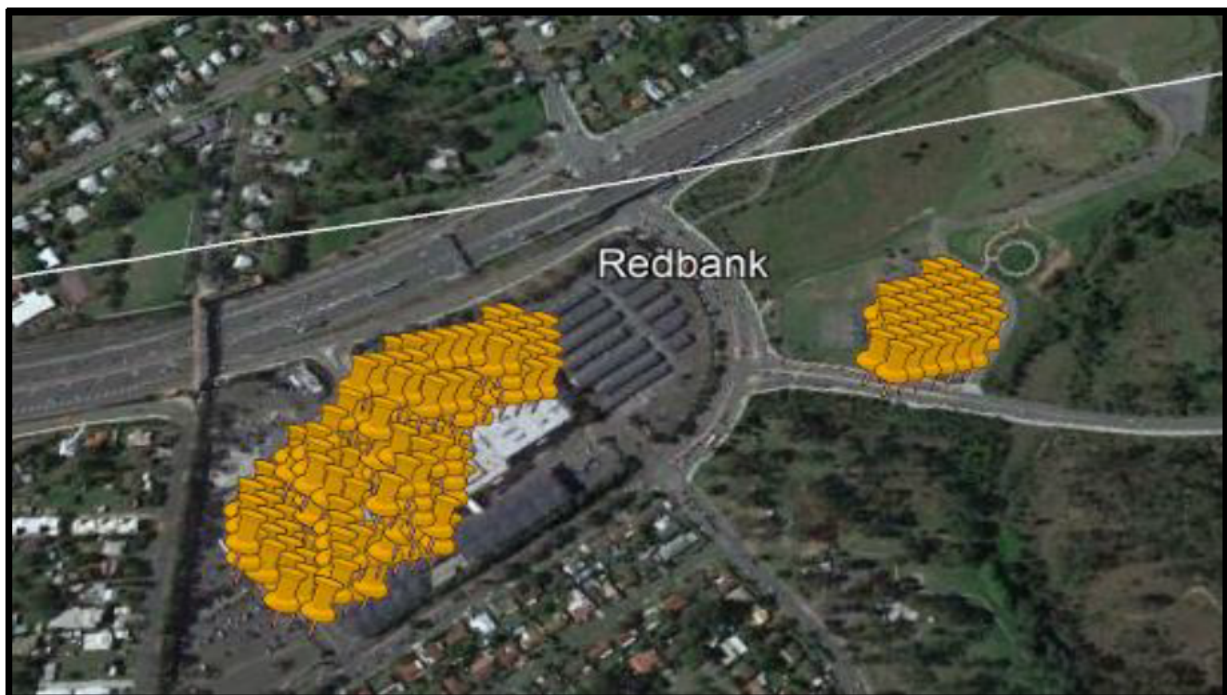


Figure 24 Location of >0.97 coherence over time, Redbank plaza.

4.2.1 15-Nov-2015 to 19-Apr-2016

The first interferogram assessed was for the period between November 2015 and April 2016. This image had a coherence of 0.8215 and a perpendicular baseline of -50.278m. It can be seen in the figure below that an approximate movement for some of the area is around the 0.002 to -0.004 meters. Therefore, it can be seen that very little movement has occurred across the area of interest and no further integration was made.

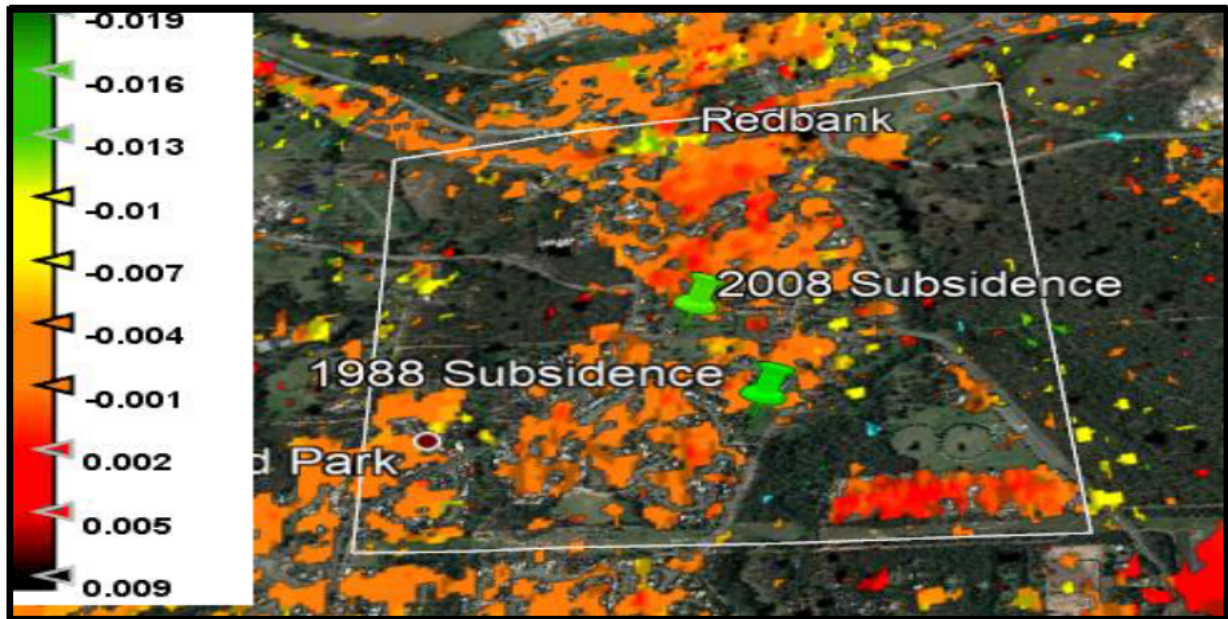


Figure 25 Results Nov15-Apr16 White polygon represents area of interest, a coherence mask of 0.4 has been applied to the image.

4.2.2 19-Apr-2016 to 03-Dec-2016

The next period to be assessed is from April 2016 to December 2016, this image had an expected coherence of 0.763 and perpendicular baseline of 42.7088m. The following figure showing the area of interest and the movement throughout it is again minimal. It can be seen there are small pockets of differences however these are not of large enough area to be of interest and could potentially be attributed to other factors given their proximity to vegetation rather than phase stable points. Therefore, it can be satisfied for this project no significant change or events have occurred throughout this period and no further investigation was needed.

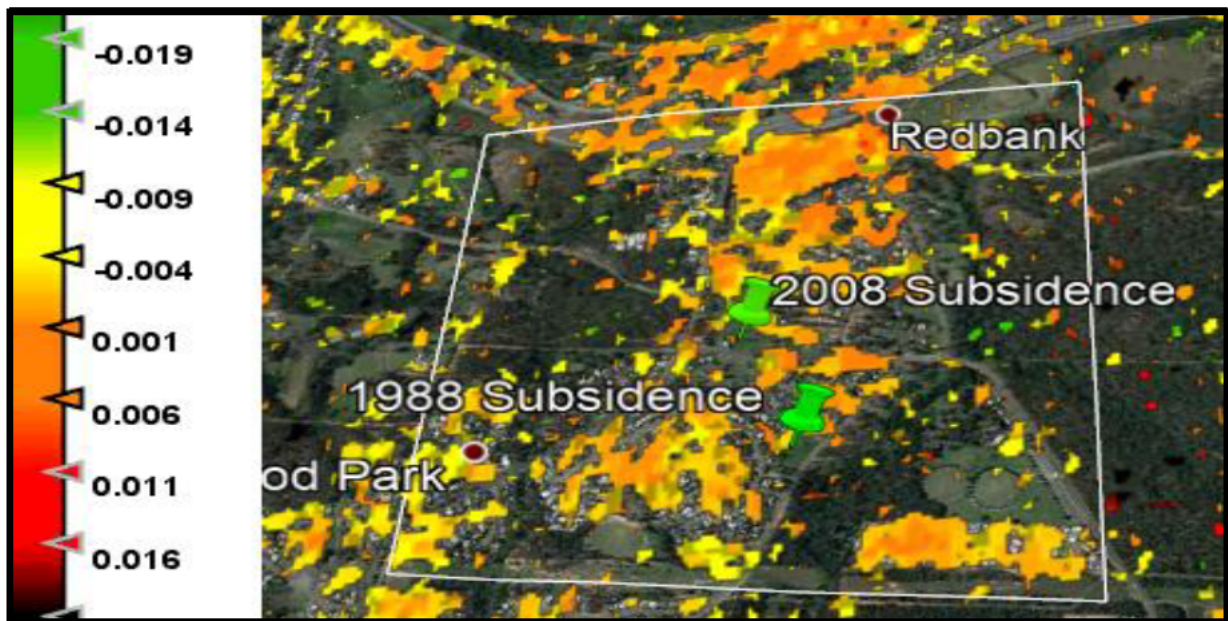


Figure 26 Results Apr16 - Dec16 coherence masking of 0.4 was used for the output of this image.

4.2.3 03-Dec-2016 to 13-Jun-2017

The next assessment time is from December 2016 to June 2017, this image has an expected coherence of 0.795 with a perpendicular baseline of -41.617m. The figure below depicts the area has had some minor movement of around 0.003 meters, although there are some small patches of difference and could possibly be contributed to errors from the time difference in the images. Another alternative is that could involve some error from trees which maybe deciduous resulting in the difference from summer to winter period. This again does not highlight any points where subsidence is occurring, therefore no further investigation was undertaken.

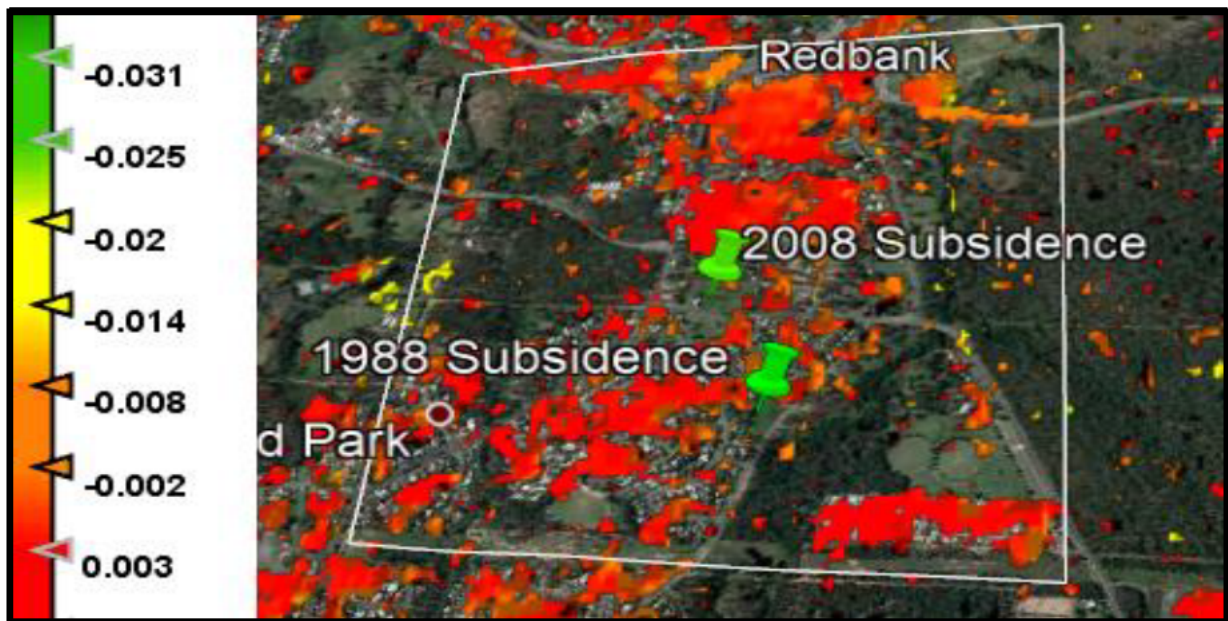


Figure 27 Results for Dec16 - June17

4.2.4 13-Jun-2017 to 22-Dec-2017

This interferogram is from June 2017 to December 2017 it has an expected coherence of 0.763 and a baseline of -86.304m. The below figure shows that again very little movement has occurred throughout the area for this period. The average movement was approximately 0.004 meters throughout the area and is consistent with all previous images showing the area is stable through this time. Indicating the site is remaining stable with only normal variations.

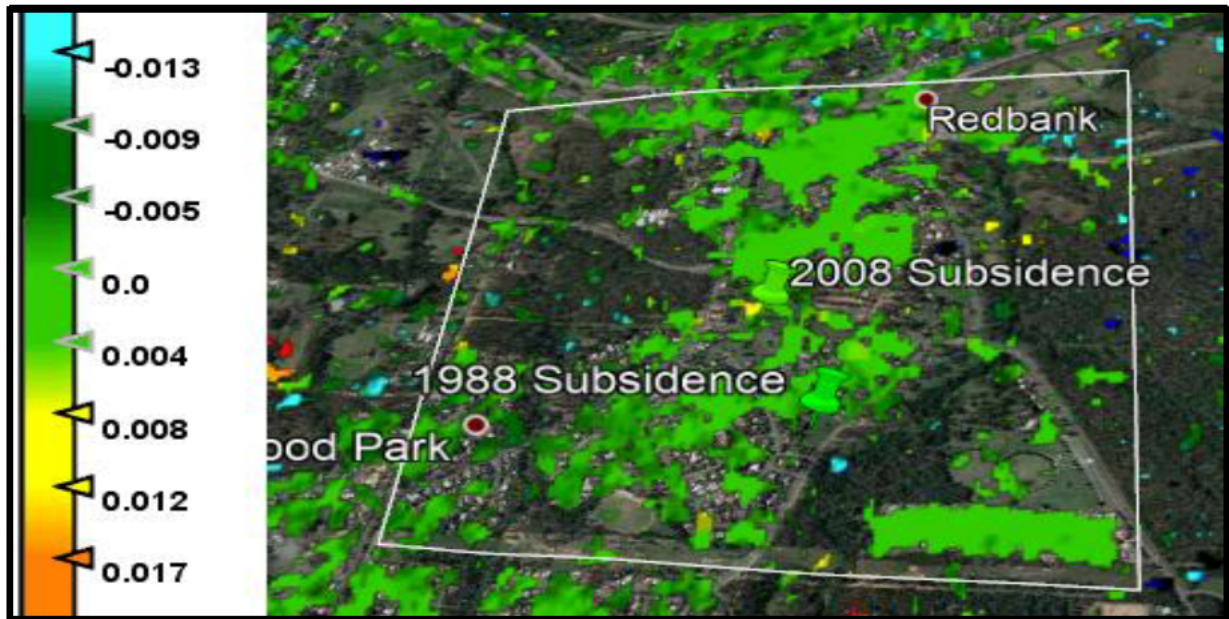


Figure 28 Results for Jun17 - Dec17

4.2.5 22-Dec-2017 to 20-Jun-2018

This interferogram covers the period of December 2017 to June 2018 with an expected coherence of 0.783 and a perpendicular baseline of 70.712m. It can be seen in the figure below that there has been some movement in the area through this period. However, the change is relatively small averaging 0.004m of total change throughout the area, and no unexpected results have occurred. There were some areas which were highlighted showing independent movement. However, as the change is small, no further processing was used as part of this project.

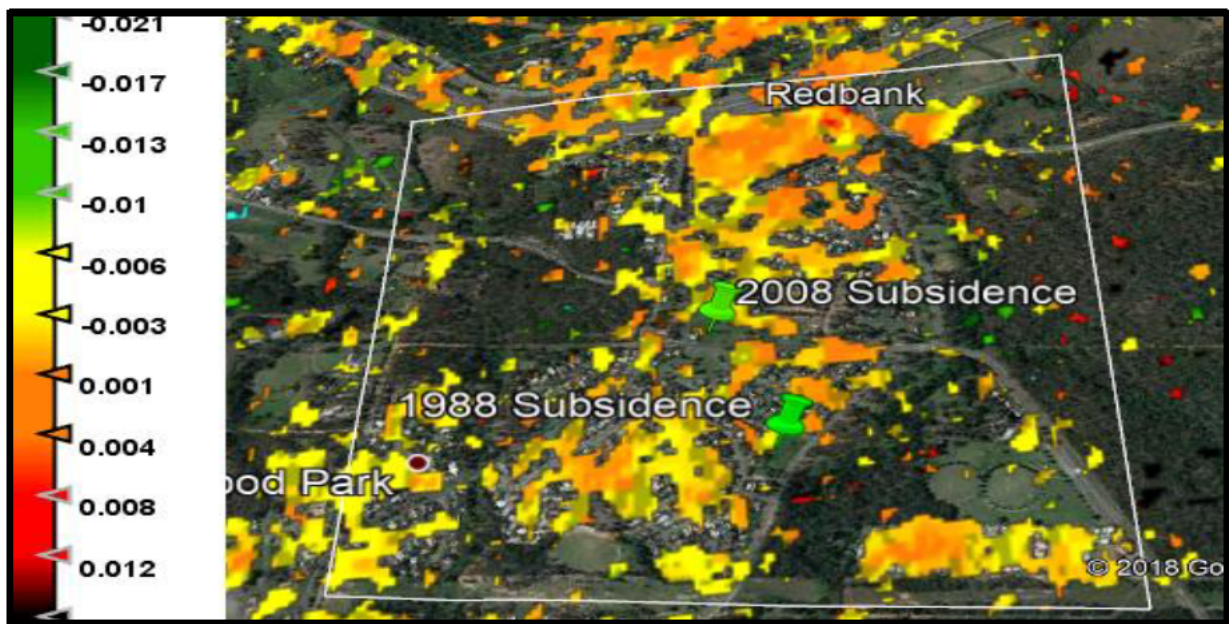


Figure 29 Results for Dec17 - June18

4.2.6 20-Jun-2018 to 29-Dec-2018

This interferogram covers the remainder of the time of the project being June 2018 to December 2018, it has an expected coherence of 0.773 and a perpendicular baseline of 72.802m. This interferogram shows that some movement has occurred throughout the time period, which is not consistent with the other generated interferograms as it is in spots of large area. This is seen in the bottom right hand portion where the blue shade is lighter, this is approximately an average of 0.07 meters of uplift. Given the lack of demonstrated movement in the previous time periods this is time was deemed worthy of further investigation. This image was exported to excel where areas of movement greater than 0.006m were able to be converted to csv to plot the points to identify the area this can be seen in Figure 31. Given this unusual movement of change to the rest of the image and that it was an uplift where any expected movement was expected to be subsidence.

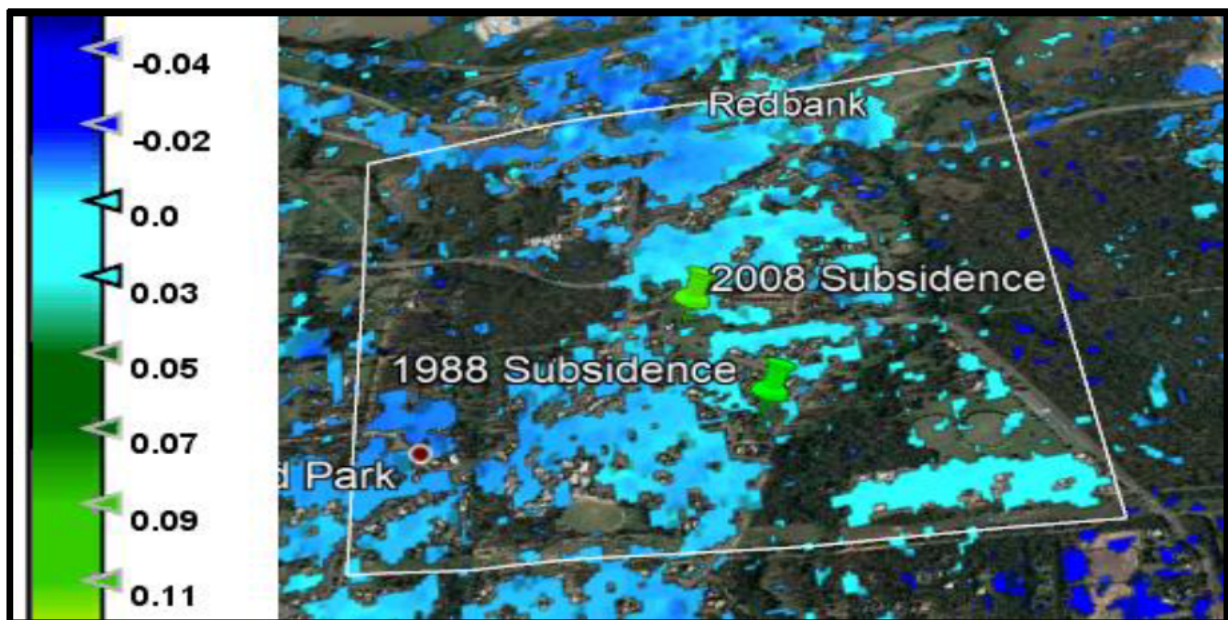


Figure 30 Results for Jun18 - Dec18

It should also be noted that this change has occurred over the area where mining has occurred in the past, unlike the area surrounding previous subsidence it cannot be confirmed if remediation works to stabilise

the ground have been undertaken. Further interferograms were generated to shorten temporal error and increase coherence, to determine when this change occurred.

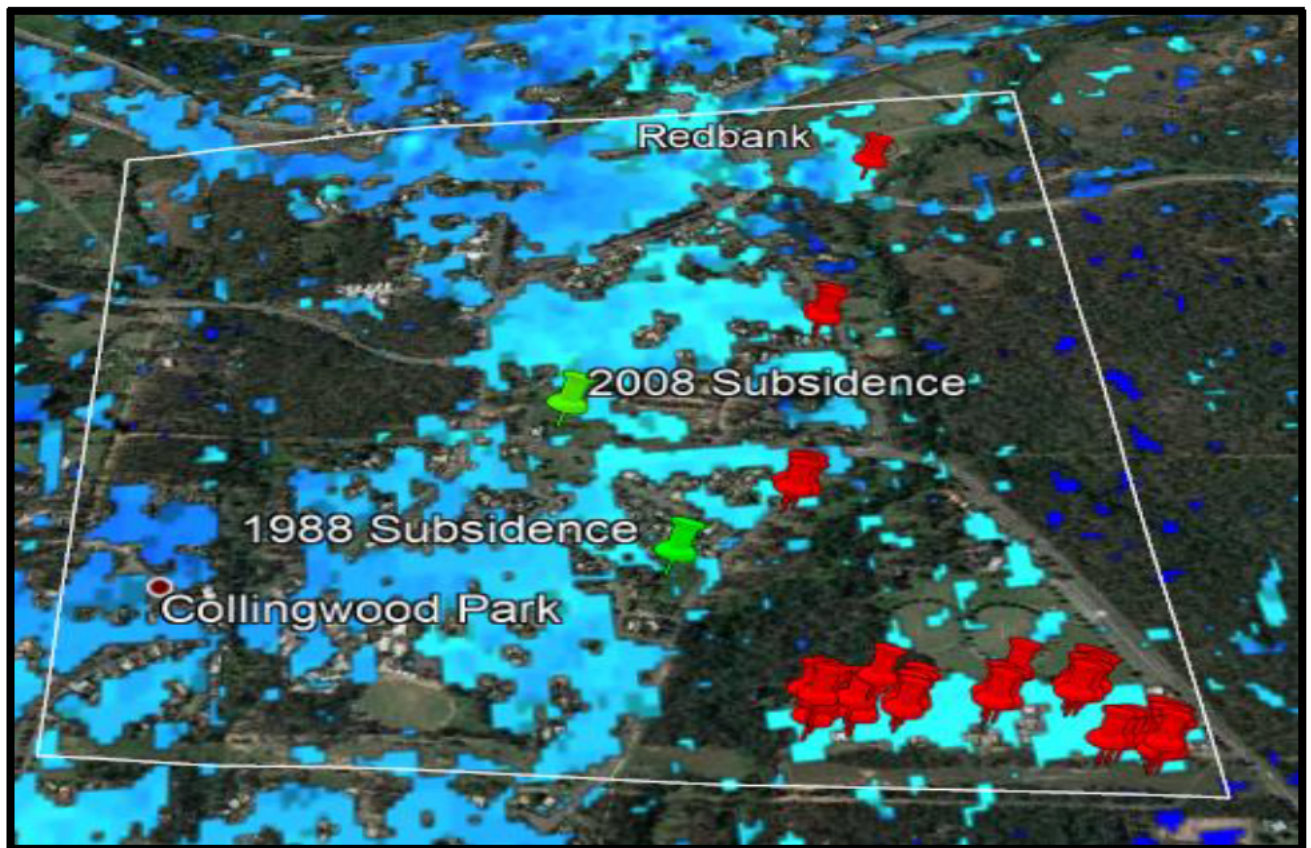


Figure 31 Area of movement $>0.006m$ with coherence value >0.6 shown by red pins

4.2.7 20-Jun-2018 to 18-Oct-2018

Following on from the above results a further image was selected being 18 October 2018, this was used to generate an interferogram with 20 June 2018 being the selected master. This interferogram had a perpendicular baseline of -120.0006 and expected coherence of 0.8143. The perpendicular baseline is getting towards the higher end of the useable range it is still within tolerance. The image shows very minimal movement for the area over this period. It also indicates that the movement detected previously would be expected in the following interferogram.

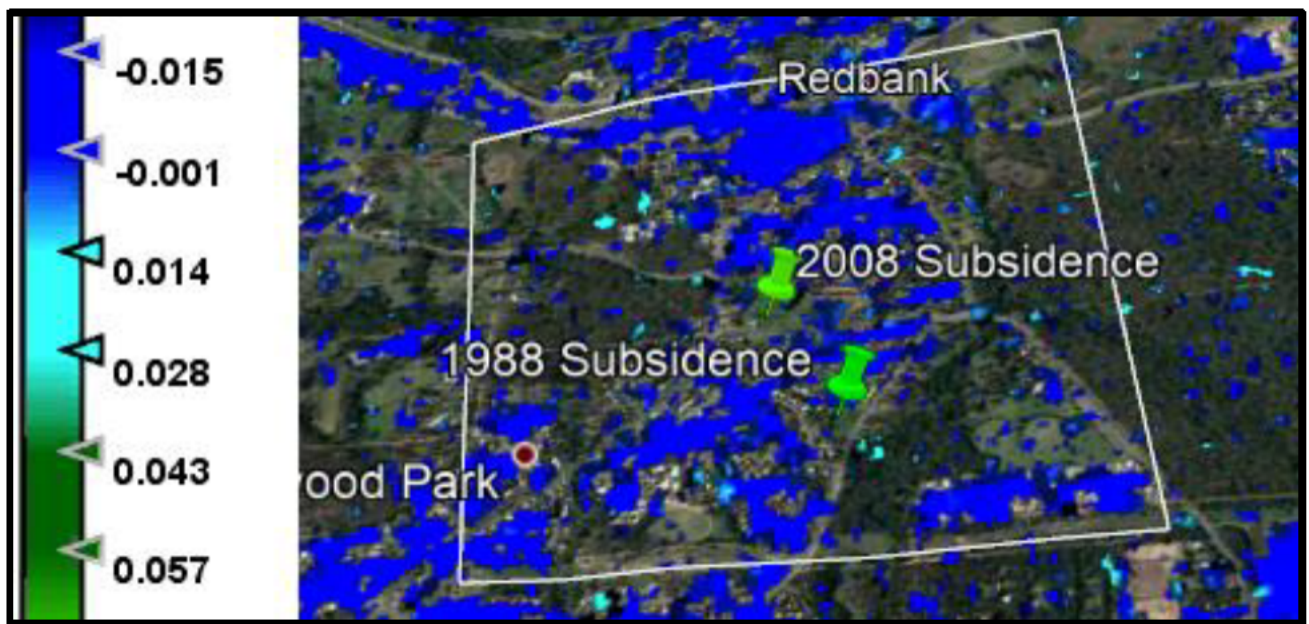


Figure 32 Results for Jun18 to Oct18

4.2.8 18-Oct-2018 to 29-Dec-2018

This interferogram was generated using October 18 image as the master and December 18 as the slave image. The interferogram had a perpendicular baseline of -71.999 meters and expected coherence of 0.9113. This interferogram generated result indicating the area had an average uplift of 0.008 metres in the area indicated in Figure 34 below. This image also indicates this has occurred in further areas throughout the site, given the decreased time period and increase in coherence it can be expected to have enhanced results. The main area is located in the bottom right of the image and this difference is also present in the June to December image.

The image indicates that the movement shown in Figure 30 has occurred during this time period, the two interferograms are showing a very similar result to the each other. This is demonstrated by the red pins in both Figure 31 and Figure 34. Whilst the second image has shown further movement in some of the surrounding area which is due to the shorter temporal baseline increasing the coherence.

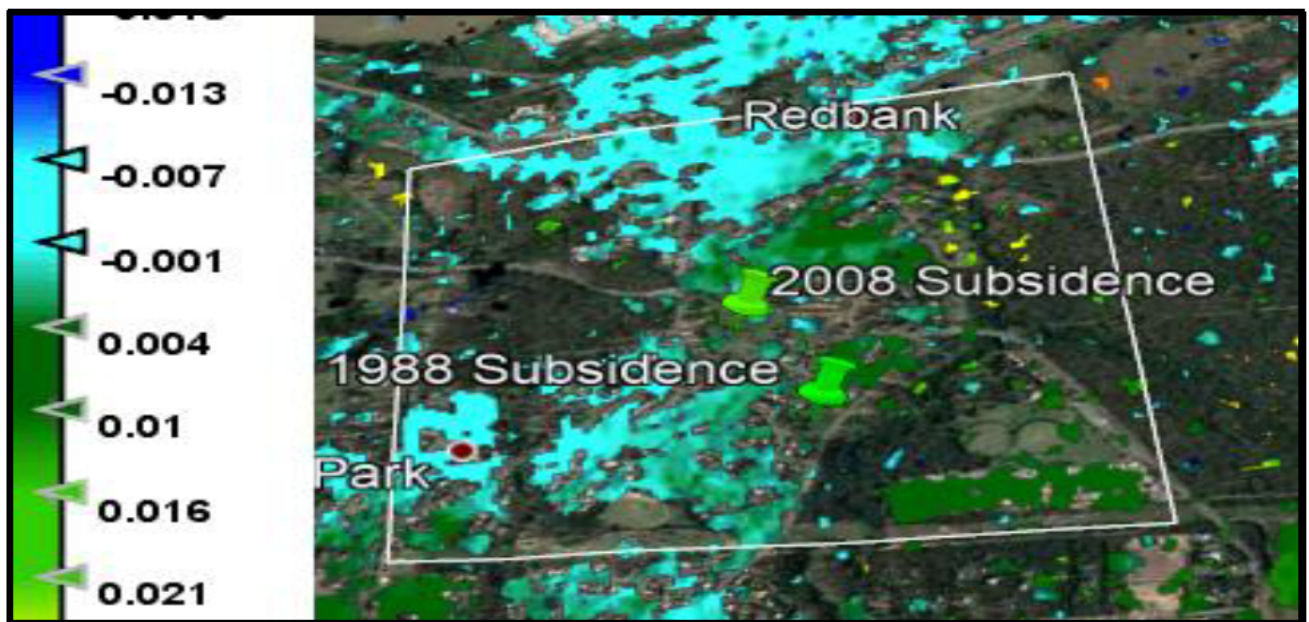


Figure 33 Results for Oct18 to Dec18

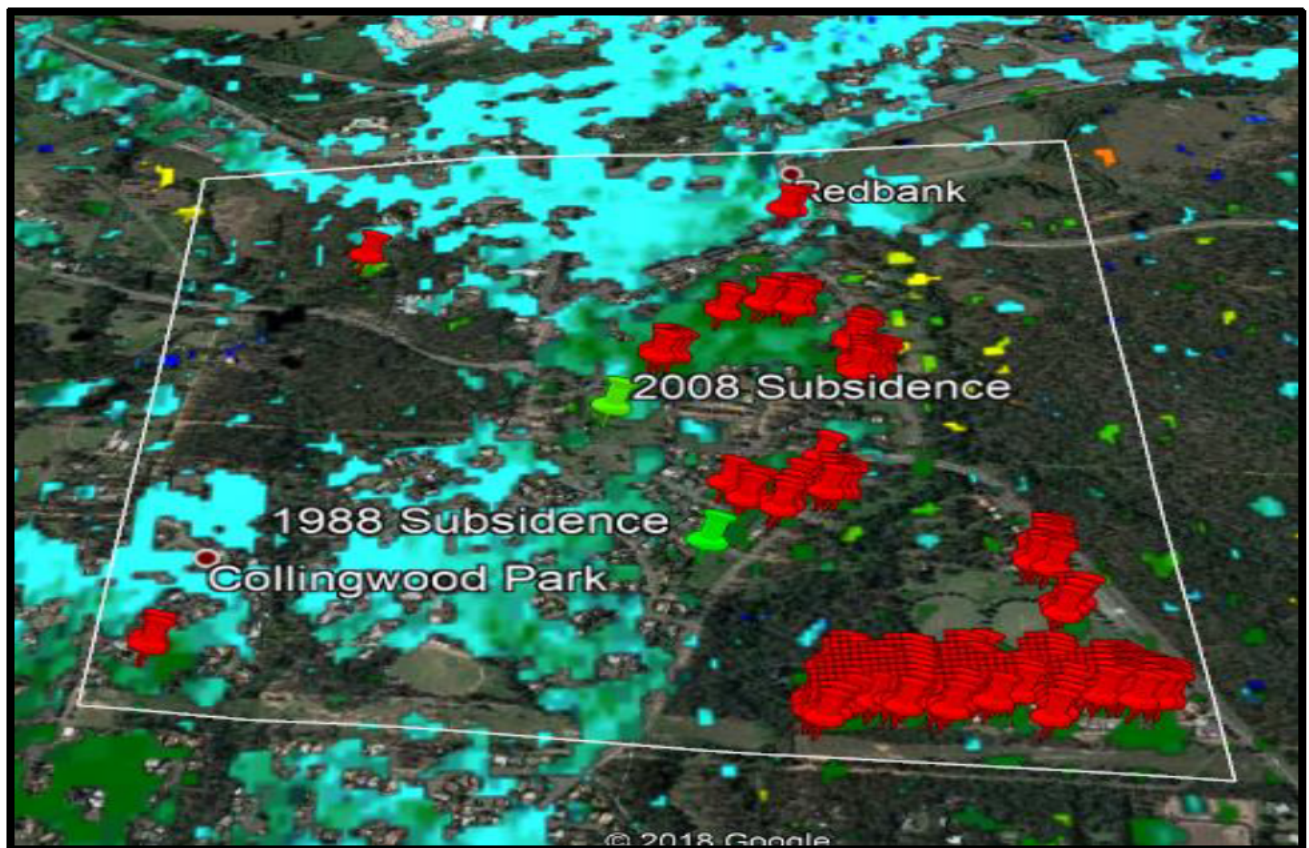


Figure 34 Area of movement $>0.006m$ with coherence value >0.6

4.3 Conclusion

Whilst it was expected that any movement found in the area would be of a subsiding nature this was not the case as discussed above. There are some factors which need to be considered when interpreting the results of this project. As this was conducted over a long period of time it would have been beneficial if the time had been available to produce further interferograms to reduce the sources of errors and increase coherence, however the amount of data generated per interferogram was also a limiting factor. This project would have benefited greatly with the use of field data to determine movement for comparison and provide GCP which had known movements. However, as the nature of this project was done in a historical sense in order to obtain data and no going monitoring occurs this was not achievable. It should also be taken into consideration the vegetation in the area could have affected some of the results during processing as some of the steps relies on the data of adjacent pixels. The atmospheric affect has been accounted for through filtering and removal of the displacement value using a high coherent point in the image. Whilst some previous research indicates this is an appropriate method, they all agree that using GPS or other more reliable data is of benefit to the result.

These results provide an indication that this method is useful for the intended purpose, projects of this nature would benefit through the use of the more advanced techniques to provide more accuracy and confidence with the results.

5 Conclusion and Further Research

5.1 Conclusion

In conclusion this project has meet its intended aims and objectives which are outlined in Appendix A. This method was useful in the detection and monitoring of land surface movement throughout the selected site of Collingwood Park, west of Brisbane City. However, unfortunately time did not permit for the development of a prediction model to be undertaken.

Through a literature review of past research and information available various sources such as ESA the project meet objective 1 and 4. Objective 2 was executed through the undertaking of online tutorials to familiarise with the programme and aided in the development of the methodology. Through meeting these objectives, they formed an integral part of the project's success. As it was these objectives which formed the projects methodology, where errors could be expected and image selection. The errors where identified and eliminated as best as possible with the programme available.

Objective 3 was one of the initial objectives to be met, this was done in consultation with the academic supervisor. It was chosen as it has potential to be an area which would benefit highly from this type of research. Another factor was that it has experienced subsidence events in the past, due to it being situated over a disused underground coal mine.

Objectives 6 and 7 were obtained in chapter 4 and chapter 5, the results were analysed through the produced velocity map and through the exporting of them to excel for further integration and display on Google Earth. They were imported to Google Earth for the purpose of understanding where the results had occurred and what the nature of the reflection source was, and if it could be in error such as areas of vegetation or construction.

The project used several data sets between the period of November 2015 to December 2018 acquired by the Sentinel 1A satellite which is part of the broader earth observation mission Copernicus. These data sets were obtained through Alaskan Satellite Facility Vertex system. The generated results indicate that no significant subsidence event had occurred during this time period and the area remained reasonably stable to June 2018. The period June 2018 to December 2018 the results do indicate some parts of the suburb had experienced some movement averaging around 0.008 meters for that areas. Upon further processing it was indicated that this had occurred somewhere in the period of October to December 2018, this result was surprising as any movement in the area was expected to be subsidence.

5.2 Further Research

Areas of further research specific to this project include; validation of atmospheric effect removal, using more advanced techniques such as PSI or SBAS, automating the processing of data, using online cloud based processing and data storage to overcome the restriction given by the enormous amount of data generated. Further processing of further interferograms with closer time periods would also be beneficial. There is still the opportunity and need to undertake research in the future modelling of areas where movement is occurring. Another area that could be researched is the integration of soil movement from reactive soils and the effects of rainfall on the data.

Other areas relating to the InSAR technique and data which could be researched include; infrastructure monitoring such as road, pipelines, rail and dams, the monitoring of mine sites and other extractive industries where subsidence is caused. The GRD images could be taken advantage of for research into monitoring of forest growth, floods and soil erosion monitoring.

6 References

Alaskan Satellite Facility, 2019, *ASF Data Search Vertex*, SLC SAR datasets, NASA, Alaska Satellite Facility, Fairbanks Alaska, viewed 21 May 2019 <<https://search.asf.alaska.edu/#/?flightDirs=&zoom=3¢er=147.30468749999994,-43.834526782236814>>

Chatterjee, R S, Thapa, S, Singh K B, Varunakumar, G & Raju, EVR 2015, 'Detecting, mapping and monitoring of land subsidence in Jharia Coalfield, Jharkhand, India by spaceborne differential interferometric SAR, GPS and precision levelling techniques', *Journal of Earth System Science*, vol. 124, no. 6, pp 1359-1376

European Space Agency, 2012, *Sentinel -1: ESA's Radar Observatory Mission for GMES Operational Services*, ESA Communications, Netherlands.

European Space Agency, N.D, SNAP in programme help guide.

Ferretti, A, Monti-Guarnieri, A, Prati, C & Rocca, F, 2007, *InSAR Principles: Guidelines for SAR Interferometry Processing and Interpretation*, ESA Publications, Netherlands.

Fielding, E, N.D, *Introduction to SAR Interferometry*, NASA, Applied Remote Sensing Training, viewed 15 April 2019, <<https://arset.gsfc.nasa.gov/sites/default/files/disasters/SAR-17/Session4-SAR-English.pdf>>

Ge, L, Chang, H-C & Rizos, C 2007, 'Mine Subsidence Monitoring Using Multi-source Satellite SAR images', *Photogrammetric Engineering & Remote Sensing*, vol. 73, no. 3, pp 259-266

Giuli, D 1966, 'Polarization Diversity in Radars', *Proceedings of the IEEE*, vol.74, no.2, pp.245-269.

Guoqing, Y & Jingquin, M 2008, 'D-InSAR Technique for Land Subsidence Monitoring', *Earth Science Frontiers*, vol. 15, no. 4, pp 239-243

Ipswich City Council: *Planning Scheme Fact Sheet no.2*, 2008, viewed 5 March 2019, https://www.ipswichplanning.com.au/data/assets/pdf_file/0016/1960/ips_fact_sheet_2.pdf

Ipswich City Council (2018), *Ipswich planning Scheme Overlay – OV3 Mining Influence Areas*, KML file, Australian Government, Digital Transformation Agency, viewed 20 March 2019, <<https://data.gov.au/dataset/ds-dga-03baae2d-d64d-4c6b-b8d4-9750f571c055/details?q=>>

McClusky, S & Tregoning, P 2013, *Background paper on subsidence monitoring and measurement with a focus on coal seam gas (CSG) activities*, The Australian National University, Canberra

Ng, AH-M, Ge, L & Li, X 2014, 'Assessment of land subsidence in the Gippsland Basin of Australia using ALOS PALSAR data', *Remote Sensing of Environment*, vol. 159, pp. 86-101

Ng, A H-M, Ge, L, Yan, Y, Li, X, Chang, H-C, Zhang, K & Rizos, C 2010, ' Mapping accumulated mine subsidence using small stack of SAR differential interferograms in the Southern coal field of New South Wales, Australia', *Engineering Geology*, vol. 115, pp. 1-15

Osmanoglu, B, Sunar, F, Wdowinski, S & Cabral-Cano, E 2015, 'Time series analysis of InSAR data; Methods and Trends', *ISPRS Journal of Photogrammetry and Remote Sensing*, vol. 115, pp. 90-102

Parker, AL, Filmer, MS & Featherstone, WE 2017, 'First Results from Sentinel-1A InSAR over Australia: Application Perth Basin', *Remote Sensing*, vol. 9, no. 3

Pinel, V, Poland, M.P & Hooper, A, 2014, 'Volcanology: Lessons learned from Synthetic Aperture Radar imagery', *Journal of Volcanology and Geothermal Research*, vol. 289, pp. 81-113.

Prats-Iraola, P, Scheiber, R, Marotti, L, Wollstadt, S & Reigber, A, (2012), 'TOPS Interferometry With TerraSAR-X', *IEEE Transactions on Geoscience and Remote Sensing*, vol.50, no, 8, pp 3179-3188.

Radar Course 2, ERS Radar Courses, European Space Agency, viewed 2 April 2019, <https://earth.esa.int/web/guest/missions/esa-operational-eo-missions/ers/instruments/sar/applications/radar-courses/content-2/-/asset_publisher/qIBc6NYRXfnG/content/radar-course-2-parameters-affecting-radar-backscatter>

Schneider, RZ & Papathanassiou, K 2007, 'Pol-DinSAR: Polarimetric SAR Differential Interferometry Using Coherent Scatters', *IEEE International Geoscience and Remote Sensing Symposium Proceedings*, pp.196-199

Shen, B, Alehossein, H, Poulsen, B, Huddleston-Homes, C, Zhou, B, Luo, X, Wang, H, Qin, J, Duan, J, Jecny, Z, Van de Werken, M & Williams, D, *Collingwood Park Mine Remediation – Subsidence control using fly ash backfilling*, Report no. EP-105068, CSIRO Earth Science and Resource Engineering, Queensland

Smith, L 2002, 'Emerging Applications of Interferometric Synthetic Aperture Radar (InSAR) in Geomorphology and Hydrology', *Annals of the Association of American Geographers*, pp 385-398

Sousa, JJ & Bastos, L 2013, 'Multi-temporal SAR interferometry reveals acceleration of bridge sinking before collapse', *Natural Hazards and Earth System Sciences*, pp.659-667

The principles of InSAR, 2012, mapping ground movement from space, Tunnel Talk, viewed on 15 April 2019, < <https://www.tunneltalk.com/New-Products-Apr12-Altamira-showcases-satellite-ground-movement-technology.php>>

UNAVCO, 2018, *Synthetic Aperture Radar (SAR) Satellites*, UNAVCO, Boulder, Colorado., viewed 22 April 2019, < <https://www.unavco.org/instrumentation/geophysical/imaging/sar-satellites/sar-satellites.html>>

Van Zyl, J & Kim, Y 2011, *Synthetic Aperture Radar Polarimetry*, John Wiley & Sons, Hoboken, New Jersey.

Ygue-Martinez, N, Prats-Iraola, P, Brcic, R, Shu, R, Geudtner, D, Eineder, M & Bamler, R, 2016, 'Interferometric Processing of Sentinel-1 TOPS-Data', *IEEE Transactions on Geoscience and Remote Sensing*, vol 54, no 4, pp 2220-2234

Yang, H-L & Peng, J-H 2014, 'Monitoring Urban Subsidence with Multi-master Radar Interferometry Based on Coherent Targets', *Indian Society of Remote Sensing*, vol 43, no 3, pp 529-538

Zhou, X, Chang, N-B & Li, S 2009, 'Applications of SAR Interferometry in Earth and Environmental Science Research', *Sensors*, no 9, pp 1876-1912

Appendix A

ENG4111/4112 Research Project

Project Specification

For: Jacob Cormick

Title: Land Subsidence Detection and Monitoring Using InSAR in Australia

Major: Surveying

Supervisor: Dr Zahra Gharineiat

Enrolment: ENG4111 – ONC S1, 2019

ENG4112 – ONC S2, 2019

Project Aim: To investigate the use of InSAR for detection and monitoring of land subsidence in Australia.

Programme: Version1, 16th March 2019

- Research the existing use of InSAR in the detection and monitoring of land subsidence.
- Establish background knowledge on the required processing techniques and software.
- Identify a suitable area to conduct the monitoring, using a site where subsidence events are known to occur.
- Research and identify possible error sources with the using InSAR for subsidence, use previous SAR as validation.
- Obtain the appropriate data from the European Space Agency (ESA).
- Analyse results from the SAR images to draw conclusion of the subsidence in selected area.
- Display the obtained results in an easily interpretable visual model.

If time and resources permit:

- Develop a model for prediction of future land subsidence events

Appendix B

This appendix provides an example of the data when exported to excel this is for the period of November 2015 to April 2016.

Longitude	Latitude	Intensity_ifg_VV_15Nov2015_19Apr2016	Phase_ifg_VV_15Nov2015_19Apr2016	coh_IW1_VV_15Nov2015_19Apr2016	Unw_Phase_ifg_15Nov2015_19Apr2016_VV	displacement_VV_slv1_15Nov2015	Absolute displacement
152.86169603375203	-27.60427797665587	1.1874457E30	3.0063996	0.52183276	-3.2767859	0.014463159	-9.6284074E-4
152.8618224267125	-27.60427797665587	6.7866776E29	-3.0041013	0.57111746	-3.004102	0.01325958	-0.0021664198
152.86194881967296	-27.60427797665587	1.0034143E30	-2.069426	0.5153626	-2.959793	0.013064008	-0.002361992
152.86207521263344	-27.60427797665587	1.5758679E30	0.9982026	0.4202997	-3.213339	0.014183116	-0.0012428839
152.8628335703963	-27.60427797665587	2.560941E30	-2.1347249	0.5016538	-3.124158	0.013789486	-0.0016365139
152.8629599633568	-27.60427797665587	4.124765E30	-3.0565715	0.6197366	-3.056572	0.013491173	-0.0019348267
152.86308635631727	-27.60427797665587	5.55025E30	-1.943645	0.6562887	-3.116347	0.01375501	-0.0016709896
152.86321274927772	-27.60427797665587	5.446107E30	3.0252225	0.6700861	-3.2579641	0.014380083	-0.0010459166

152.863339142 2382	- 27.604277976 65587	4.575862E30	2.9588616	0.64110166	-3.3243244	0.014672985	- 7.530147E -4
152.863465535 19869	- 27.604277976 65587	4.3092454E30	2.95814	0.5139809	-3.3250463	0.014676172	- 7.498277E -4
152.863591928 15917	- 27.604277976 65587	8.3234295E30	2.8542166	0.50201553	-3.4289694	0.015134871	- 2.91129E- 4
152.863718321 11962	- 27.604277976 65587	1.2904044E31	2.8193138	0.67041004	-3.4638722	0.015288925	- 1.370752E -4
152.863844714 0801	- 27.604277976 65587	1.3088501E31	2.7685757	0.757309	-3.51461	0.015512873	8.687342E -5
152.863971107 04058	- 27.604277976 65587	1.7845853E31	2.7319052	0.80936664	-3.5512807	0.01567473	2.4873076 E-4
152.864097500 00107	- 27.604277976 65587	3.5809642E31	2.6910717	0.8274724	-3.5921144	0.015854964	4.2896403 E-4
152.864223892 96155	- 27.604277976 65587	1.870885E31	2.7824428	0.6685687	-3.5007434	0.015451669	2.5668762 E-5
152.864350285 922	- 27.604277976 65587	2.6601383E31	2.481982	0.5637895	-3.8012037	0.016777849	0.0013518 488
152.864476678 88248	- 27.604277976 65587	3.7470056E31	2.43406	0.58414906	-3.8491254	0.016989365	0.0015633 652

152.864603071 84296	- 27.604277976 65587	3.211319E31	2.19653	0.6127666	-4.086656	0.018037785	0.0026117 847
152.864729464 80345	- 27.604277976 65587	1.4884073E31	1.8930408	0.63505995	-4.390146	0.019377334	0.0039513 34
152.864855857 76393	- 27.604277976 65587	2.4335919E31	2.104015	0.67094445	-4.17917	0.018446125	0.0030201 25